Results in Engineering 27 (2025) 107097

Contents lists available at ScienceDirect

Results in Engineering

journal homepage: www.sciencedirect.com/journal/results-in-engineering

Numerical exploration and relational impact ranking of critical parameters in 3D PV module studies

Yassine El Alami [a], Elhadi Baghaz [a,b], Rehena Nasrin [c], Charaf Hajjaj [a], Mohammadi Benhmida [a], Khaled M. Al-Aribe [d], Adnan Ibrahim [e,*]

[a] Laboratory of Electronics, Instrumentation and Energetic, Faculty of Sciences, Chouaïb Doukkali University, B.P. 20, El Jadida, Morocco
[b] Research Center, High Studies of Engineering School, EHEI, Oujda, Morocco
[c] Department of Mathematics, Bangladesh University of Engineering and Technology, Dhaka-1000, Bangladesh
[d] Department of Mechanical and Industrial Engineering, Abu Dhabi University, Abu Dhabi PO Box 59911, United Arab Emirates
[e] Solar Energy Research Institute, Universiti Kebangsaan Malaysia, 43600, Bangi, Selangor, Malaysia

ARTICLE INFO

Keywords:
Three-dimensional numerical modeling
PV module
Dust accumulation
Grey relational analysis method
Temperature and efficiency

ABSTRACT

The performance of photovoltaic modules is susceptible to environmental conditions, which often leads to efficiency losses in real-world installations. It is therefore essential to develop accurate forecasting tools in order to better understand these effects and improve the reliability and sustainability of solar systems. In this study, a three-dimensional numerical model was developed and experimentally validated to accurately predict the temperature and performance of photovoltaic modules. This approach offers significant advantages over traditional models, providing a more realistic and comprehensive representation of module behavior under different conditions. The model was used to assess the influence of several factors, including ambient temperature, dust accumulation, wind speed, solar irradiance, and module tilt angle, on panel temperature, power generation, and efficiency. To quantify the relative impact of each of these parameters on module performance, the Grey Relational Analysis method was applied. Dust accumulation is the primary issue causing a significant decrease in temperature and power output compared to clean PV, primarily due to reduced glass transmission. For example, a 45 g/m^2 dust deposit decreases module temperature by 1.18 °C, reduces output power by 22.605 W, and reduces efficiency by 0.073 %. Furthermore, temperature decreases as dust, wind speed, and tilt angle increase, while it rises with irradiance and ambient temperature. Power and efficiency, on the other hand, follow an opposite trend, generally decreasing with dust accumulation, irradiance, and temperature, but improving with high wind speed and optimum tilt angle.

1. Introduction

Global interest in renewable energies has fully-fledged significantly recently, fueled by the need to meet the challenges of weather variation and the rapid increase in electricity consumption [1]. Among the various sustainable solutions, solar energy occupies a privileged position due to its availability, the constant evolution of its technologies, and its increasingly competitive costs. Thanks to these advantages, PV solar power is now seen as a central pillar of the energy transition [2]. PV modules, in particular, are the key element of this technology [3,4]. Their energy yield depends directly on their ability to convert solar radiation into electricity, a process strongly influenced by their operating temperature [5,6]. Contrary to popular belief, prolonged exposure to sunlight can impair their performance. Each rise in module temperature results in a corresponding drop in conversion efficiency [7,8], estimated at between 0.05 % and 1 % per degree Celsius, accompanied by a power reduction of up to 0.3 % [9]. This thermal sensitivity represents a crucial issue for the optimization of PV installations. The sustainability of PV systems is also becoming an increasingly pressing issue. According to the International Renewable Energy Agency (IRENA), rapid growth in installed capacity will lead to a substantial volume of panels being taken out of service over the coming decades [10]. By 2030, up to 8 million tonnes of PV waste could be generated, a figure that could rise to 78 million tonnes by 2050, in connection with an estimated global capacity of 4500 GW [10]. In this context, it is crucial to better understand the thermal phenomena that affect PV modules to optimize their performance and extend their lifespan. Module temperature is not an isolated

* Corresponding author.
E-mail address: iadnan@ukm.edu.my (A. Ibrahim).

https://doi.org/10.1016/j.rineng.2025.107097
Received 27 July 2025; Received in revised form 20 August 2025; Accepted 2 September 2025
Available online 2 September 2025

Nomenclature

Abbreviation

GRD	Grey Relational Degree
EVA	Acetate ethylene vinyle
GRA	Gray relational analysis
PVT	Photovoltaic thermal
IRENA	International Renewable Energy Agency
PV	Photovoltaic
FEM	Finite element method
GRC	Gray relational coefficient
NOCT	Nominal Operating Cell Temperature
CFD	Computational fluid dynamics

Parameters

Q_t	Heat generated
T_{ted}	Tedlar temperature (°C)
A_{PV}	PV surface area (m^2)
G	Solar irradiance (W/ m^2)
T_{sky}	Sky temperature (°C)
T_{amb}	Ambient temperature (°C)
P_{PV}	Electrical power (W)
J_d	Amount of dust (g/m^2)
T_c	Cell temperature (°C)
k	Thermal conductivity ($Wm^{-1}K^{-1}$)
C_p	Specific heat ($JKg^{-1}K^{-1}$)
T_{PV}	PV panel temperature (°C)
T_g	Glass temperature (°C)

Greek Symbols

ε	Emissivity
η_{el}	Electrical efficiency (%)
ρ	Density (Kg m^{-3})
σ	Stefan-Boltzmann constant
η_{ref}	Reference efficiency
β_{ref}	Temperature coefficient
α	Absorptivity
τ	Transmissivity

parameter, but rather results from a complex set of interactions with the environment, including external temperature, irradiation, panel tilt angle, wind velocity, and dust accumulation. This is why a multi-factorial, coupled analysis of these influences is essential to accurately assess the overall impact on the temperature, power output, and electrical efficiency of PV systems.

The evolution of PV module performance has been extensively studied as a function of various environmental parameters such as irradiance, wind speed, tilt angle, ambient temperature, and dust accumulation. Wang et al. [11] analyzed the effects of various environmental parameters on the surface temperature of PV modules at low temperatures. Using grey relational analysis (GRA), they identified solar irradiance as the leading issue, shadowed by external temperature, wind speed, and humidity. Huang et al. [12] conducted an outdoor experiment to investigate the effects of irradiance, air speed, and row spacing on PV surface temperature and power output. They showed that irradiance has the greatest impact, while the effect of wide spacing remains limited once shading is avoided. Gholami et al. [13] examined the impacts of irradiance, external temperature, humidity, wind velocity, and dust gathering on PV temperature. Semi-empirical correlations validated by thermal simulations were used to effectively predict this temperature, highlighting the dominant role of irradiance and ambient temperature. Jo et al. [14] investigated the impact of solar radiation, relative humidity, surface temperature, and flow rate (specific to photovoltaic thermal (PVT) systems) on PV performance. They demonstrate that solar radiation has a significant impact on production in winter, whereas several factors act in concert in summer. Surface temperature and humidity also modulate power generation, and flow rate has a significant impact on temperature and performance in PVT systems. Keddouda et al. [15] have demonstrated that solar radiation, ambient temperature, and wind speed significantly impact the temperature of PV modules. A 100 W/m^2 increase in radiation can raise module temperature by up to 4 °C, while a 6 °C increase in ambient temperature results in a rise of around 5.8 °C. Wind speed attenuates this temperature rise. Yaman et al. [16] studied the impact of various meteorological parameters on the thermal and electrical performance of PV modules using a detailed mathematical model validated experimentally. They demonstrated that solar radiation and ambient temperature have a significant impact on cell temperature, whereas wind speed has a lesser effect. Zhao et al. [17] analyzed the impact of humidity, wind speed, particle size, and tilt angle on dust deposition on PV modules. Their results show that increasing humidity and particle size favor accumulation, while stronger wind and higher inclination reduce it. They therefore recommend optimizing the tilt angle to limit the negative effect of dust.

Various methods exist to predict PV cell temperature. One of the earliest models by Ross [18] suggested a linear relationship between temperature difference and solar irradiance, with a proportionality constant within a specific range [19]. Lasnier [20] developed a regression model to estimate module temperature based on solar radiation and ambient temperature, while Servant's [21] model incorporated wind speed, showing good alignment with experimental data. King [22] created an empirical model indicating that module temperature is influenced by solar radiation, ambient temperature, and wind speed. In a follow-up study, King et al. [23] refined this model by adding material characteristics and linking cell temperature to the backside temperature of the module.

Davis et al. [24] introduced the Nominal Operating Cell Temperature (NOCT) model, which predicts PV module temperature based solely on ambient temperature and irradiance, without considering wind speed, tilt angle, or dust buildup. Jha et al. [25] employed a heat transfer model to investigate the impact of wind speed and seasonal variation, revealing that dust-related efficiency losses are more pronounced in summer than in winter. Gu et al. [26] developed a combined thermoelectric model to improve the prediction accuracy of module temperature and output power by capturing the system's dynamic behavior. Additionally, several researchers utilized numerical simulations [27,28] to study PV module temperature, efficiency, and power output, including PVT systems [29,30]. Lu and Zhao [31] assessed the impact of dust on PV performance through computational fluid dynamics (CFD) simulations, revealing that dust reduces efficiency and that particle size is a significant factor. Dabaghzadeh et al. [32] created a 3D model to evaluate how wind speed, direction, and tilt angle affect module temperature; however, it did not account for dust buildup or variations in solar radiation.

Upon reviewing the details, it is evident that most efforts have been directed towards predicting the clean PV temperature using experimental data or traditional thermal models. Conversely, studies examining the dust effect on PV thermal performance remain limited, both in terms of number and depth of analysis. Very little research has mobilized advanced numerical tools to simulate the soiled PV temperature. Yet this approach holds great promise for exploring the joint influence of complex parameters such as irradiance, ambient temperature, wind speed, tilt angle, and the amount of dust accumulated on the module surface. Most studies to date have focused on the individual impact of certain parameters, notably air temperature [33], irradiance [34], dust accumulation [35,36], and wind speed [37], on the temperature and power output of PV modules. However, other important factors, such as the angle of inclination or the mass of accumulated dust, have not been sufficiently investigated. In particular, the interaction of these parameters and their combined effect on module temperature and electrical efficiency have not yet been thoroughly addressed. To address these gaps, this study proposes the development of a three-dimensional thermal simulation model based on the finite element method (FEM), which can accurately predict the temperature of a PV module under variable ambient conditions. This model will be validated using experimental data and will be used to conduct a detailed parametric analysis of both the individual and combined effects of each factor. Finally, to identify the most influential parameters, a multi-criteria analysis method, namely GRA, will be employed to quantify the impact of each variable on the temperature, power output, and efficiency of the PV module.

This study stands out for its major contributions and the introduction of new features in the analysis of PV modules. A 3D mathematical modeling was proposed to realistically simulate PV's thermal behavior exposed to various outdoor conditions. This model simultaneously integrates key parameters like dust gathering, panel inclination, air speed, solar radiation and temperature (ambient). The model's accuracy was confirmed by cross-validation with experimental-numerical results from the literature. Using this model, an in-depth investigation was performed to examine not only each factor's individual effect on PV temperature, power generation, module efficiency, but also the synergistic effects resulting from the combination of these parameters. This approach made it possible to identify the most significant thermal interactions. To complete the analysis, a multi-criteria evaluation method, the GRA method, was applied. This approach made it possible to assign a quantitative weight to each of the parameters studied, highlighting their respective influence on the PV module's thermal-electrical performance.

2. Methodology

2.1. PV panels composition

We used a monocrystalline PV module (supreme output 90 W) for thermal analysis. The module consists of 36 solar cells (125 *125 mm^2). The overall dimensions of the panel are 1200 mm long and 545 mm wide. Its internal structure is based on five superimposed layers (Fig. 1), arranged from back to front, each fulfilling a specific functional role. The first is a sheet of Tedlar, used as an external protective layer against moisture and environmental aggression at the rear of the module. The first layer is EVA, serving as an encapsulation material, ensuring the adhesion and mechanical stability of the internal components. The center is PV cells (monocrystalline silicon), converting solar energy into electricity. These are covered by a second layer of EVA, identical to the first, providing additional protection and holds the cells in place. On the surface, a transparent tempered glass plate forms the top layer. This provides mechanical protection for the module while allowing good transmission of solar irradiance to the cells. These layers are held together by a metal frame, ensuring the panel's rigidity and durability. However, we did not consider this frame as its deemed insignificant effect due to having relatively tiny area related to whole PV [38–39]. The thermophysical properties of each of the module's constituent layers - thickness, thermal conductivity, density, and mass heat capacity are detailed in Table 1, which serves as the basis for the numerical simulations carried out in this study.

2.2. Simulation procedure

The PV module's temperature distribution was numerically exhibited using COMSOL Multiphysics software. The approach adopted considers conduction within the PV layers, natural convection from PV's outer surface to ambient air, and thermal radiation between surfaces. For this purpose, we used "Heat transfer in solids" and "Surface-to-surface radiation" physics [41]. Solar radiation (external thermal source),

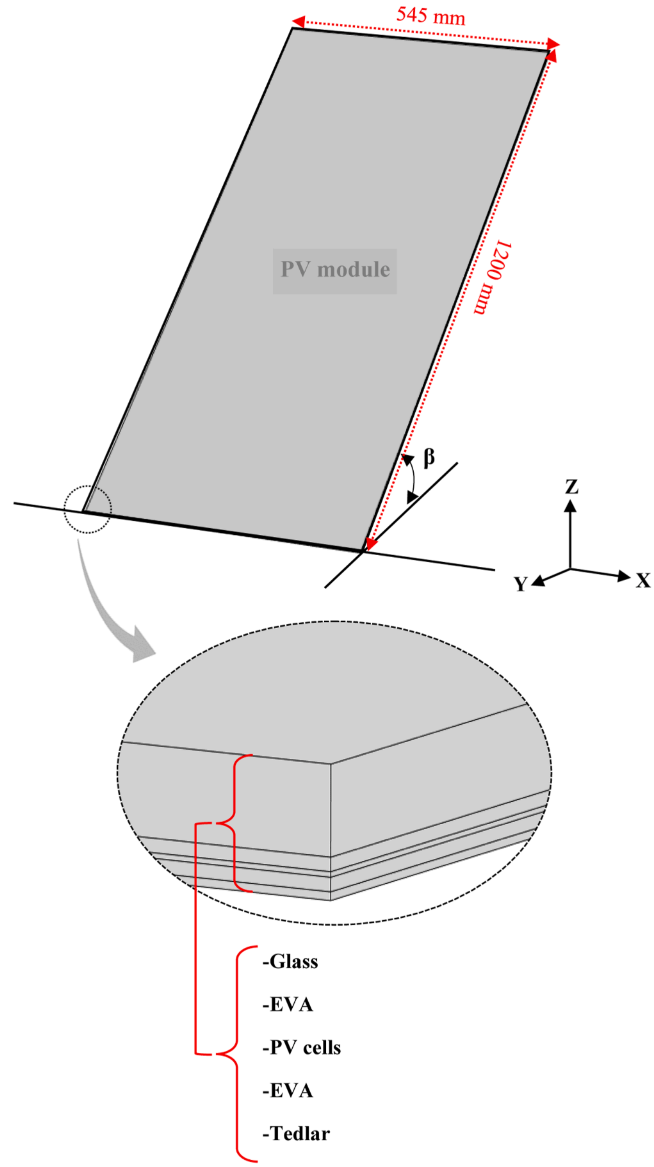

Fig. 1. PV module's structure.

applied perpendicular to the module's upper surface. It is characterized by a heat flux that varies according to the simulated irradiance. In terms of optical properties, the silicon layer and other layers were treated as opaque and transparent, respectively, with a refractive index equal to 1.50 [40,41]. Diffuse radiation was neglected, simplifying heat exchange to direct interactions between surfaces. A linear discretization technique was applied to solve the equations numerically. Finally, the simulation results were processed and analyzed using Origin 2018 software to extract thermal trends for the module.

2.3. Thermal hypotheses

Several assumptions were considered. These simplify certain aspects related to the PV module structure, ambient conditions, and other variables likely to affect the results.

- The PV module is represented as a uniform five-layer structure, neglecting the spaces between the cells (2 mm), which are insignificant compared with the total module surface area [40].
- The ambient air is assumed to have a uniform temperature around the panel, and the lateral edges of the model are assumed to be

Table 1
Materials' optical properties [38,40].

Material	Thickness (mm)	ρ (kg/m^3)	k (W/m.K)	C_p (J/kg.K)	Emissivity	Refractive index	Relative permittivity
EVA	0.50	935	0.29	2400	*	*	*
Glass	0.1–3.2	2200	1.04	750	0.85	1.5	4.2
Backsheet	0.3	1200	0.14	1250	0.92	*	*
Silicon	0.192	2329.1	163	703	0.85	3.45	11.7

*Value not relevant for simulation.

adiabatic, their contribution being negligible due to their small size [42–43].

- All the materials making up the module are considered in the absorption of solar radiation. All energy not converted into electricity by the cells is dissipated as heat [43].
- Heat transfer by radiation is modeled by assuming that the front face exchanges heat with the sky, while the rear face radiates towards the ground [43].
- Rear convection has been estimated at 50 % of front convection, taking into account less efficient heat exchange [44].

2.4. Boundary conditions

Pv's hermal modeling was presented in detail in Fig. 2, where the boundary conditions defined for the simulation are clearly specified. The diagram shows the various layers of the module and the heat exchanges between them.

The electrical energy produced by a PV cell comes from the absorption of solar photons, which also results in the release of heat. The heat generated by PV panels, energy that is not converted into electricity, is quantified by the following equation [40]:

$$Q_t = (1 - \eta_{PV}) \cdot G \cdot A_{PV} \cdot T(\%) \tag{1}$$

In this expression, η_{PV} is the efficiency of the PV module, A_{PV} is the total surface area of the module, and T (%) is the percentage of sunlight reaching the panel surface.

In a PV panel, heat mainly moves through three mechanisms: conduction, convection, and radiation. The surface exposed to the sun exchanges thermal radiation with the atmosphere, while the opposite side exchanges heat with the Earth. Radiation transfer can be quantified by the following equation [39,45]:

$$Q_{rad,1} = \varepsilon_g \cdot \sigma \cdot \left({T_g}^4 - {T_{sky}}^4\right) \cdot A_{PV} \tag{2}$$

$$Q_{rad,2} = \varepsilon_g \cdot \sigma \cdot \left({T_g}^4 - {T_{amb}}^4\right) \cdot A_{PV} \tag{3}$$

Where σ is the Stefan-Boltzmann constant, T_{PV} is the PV panel temperature, T_{amb} is the ambient temperature, T_{sky} is the sky temperature, and ε is the glass emissivity.

The studies presented in [46–47] assume that the ground temperature is identical to the ambient temperature, while the sky temperature is calculated from the following equation:

$$T_{sky} = 0.0552 \cdot T_{amb}^{1.5} \tag{4}$$

Convection is an important mode of heat dissipation between the module and its environment. The heat dissipated by this process to the ambient air is quantified by the following formula [40]:

$$Q_{conv,1} = h \cdot \left(T_g - T_{amb}\right) \cdot A_{PV} \tag{5}$$

$$Q_{conv,2} = h \cdot \left(T_{Back} - T_{amb}\right) \cdot A_{PV} \tag{6}$$

Where h represents the convective heat transfer coefficient, and T_g, T_{Back} are the temperatures of the top glass and rear surface of the PV module, respectively.

Wind speed (V) influences the module's convective heat transfer coefficient, which can be determined using the following equation [43, 48]:

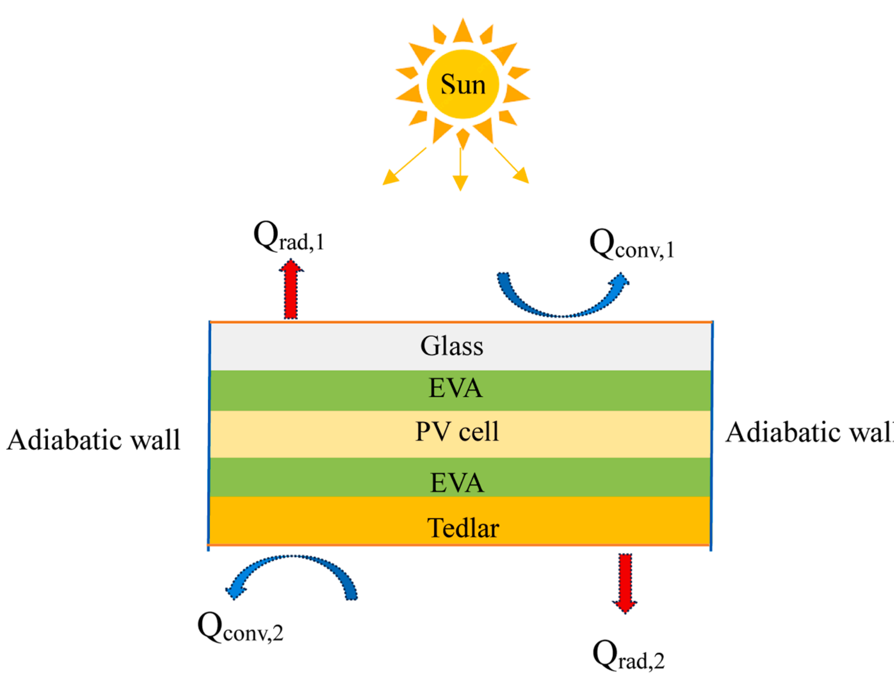

Fig. 2. Diagram of the boundary conditions used for the PV module.

$$h = 5.82 + 4.07 \cdot V \tag{7}$$

According to references [43–44,48], convective heat transfer on the rear face of the module is reduced by 50 % compared to the front face, this being attributed to less exposure to air flows and less efficient cooling.

2.5. Performance analysis

The electrical efficiency of solar cells within a PV module varies according to their operating temperature. This relationship can be quantified by the following equation, which takes into account the direct impact of temperature on the module's electrical productivity [49]:

$$\eta_{PV} = \eta_{ref} \cdot \left(1 - \beta_{ref} \cdot \left(T_c - T_{ref}\right)\right) \tag{8}$$

Where η_{ref} is the reference efficiency, β_{ref} is the temperature coefficient of the PV cell, T_c is the cell temperature, and T_{ref} is the reference temperature set at 25 °C.

The output power of a PV module is directly influenced by the temperature of its cells. Indeed, as cell temperature rises, their electrical efficiency decreases, impacting power output. This relationship between output power and cell temperature can be expressed mathematically by the following equation [38,45]:

$$P_{PV} = \eta_{ref} \cdot \tau \cdot \alpha_c \cdot G \cdot A_{PV} \cdot \left(1 - \beta_{ref} \cdot \left(T_c - T_{ref}\right)\right) \tag{9}$$

Where τ represents the transmissivity of the glass, α the absorptivity of the cells (value fixed at 0.9), and G the incident solar irradiance.

When the glass surface of a PV module is covered with dust, the amount of sunlight able to pass through is reduced. This reduction in transmittance directly affects module performance, as less radiation reaches the PV cells. Eq. (10) [9] establishes a quantitative relationship between the level of dust accumulation and glass transmittance, providing a means of accurately calculating the transmittance to be taken into account in solar panel performance analyses.

$$\tau = \tau_0 \cdot [1.01645 - 0.09885 \cdot ln(J_d + 1.18102)] \tag{10}$$

Here τ_0 and τ are transmittance of clean and dirty glass, respectively. J_d represents the amount of dust in g/m^2 affecting this transmittance.

2.6. Mesh independence study

To ensure an optimal balance between result accuracy and computational time requirements, an in-depth study of the meshing strategy was conducted. Two mesh topologies were considered for the numerical modeling of the PV system under study: an unstructured mesh based on free triangular elements, and a structured mesh composed of regularly distributed quadrilateral elements (Fig. 3). The key goal was to detect the maximum efficient mesh configuration in terms of thermal stability of results and numerical performance. Rather than focusing solely on mesh density, the evaluation also considered the mesh topology in relation to PV thermal characteristics and simulation time. This approach was applied under constant conditions (1 m/s air speed, 1000 W/m^2 radiation, and 26 °C ambient temperature). Table 2 presented results, revealed that the choice of mesh has a strong influence on calculation time, without compromising thermal accuracy above a certain level of refinement. In particular, the structured mesh exhibits better numerical efficiency, with significantly reduced simulation time, while maintaining the stability of thermal results comparable to those from a finer mesh type. This stability indicates that the solution has become mesh-independent at this stage.

In conclusion, the structured mesh with a finer mesh type was adopted for the remainder of the simulations, as it guarantees both sufficient accuracy and reasonable computation time.

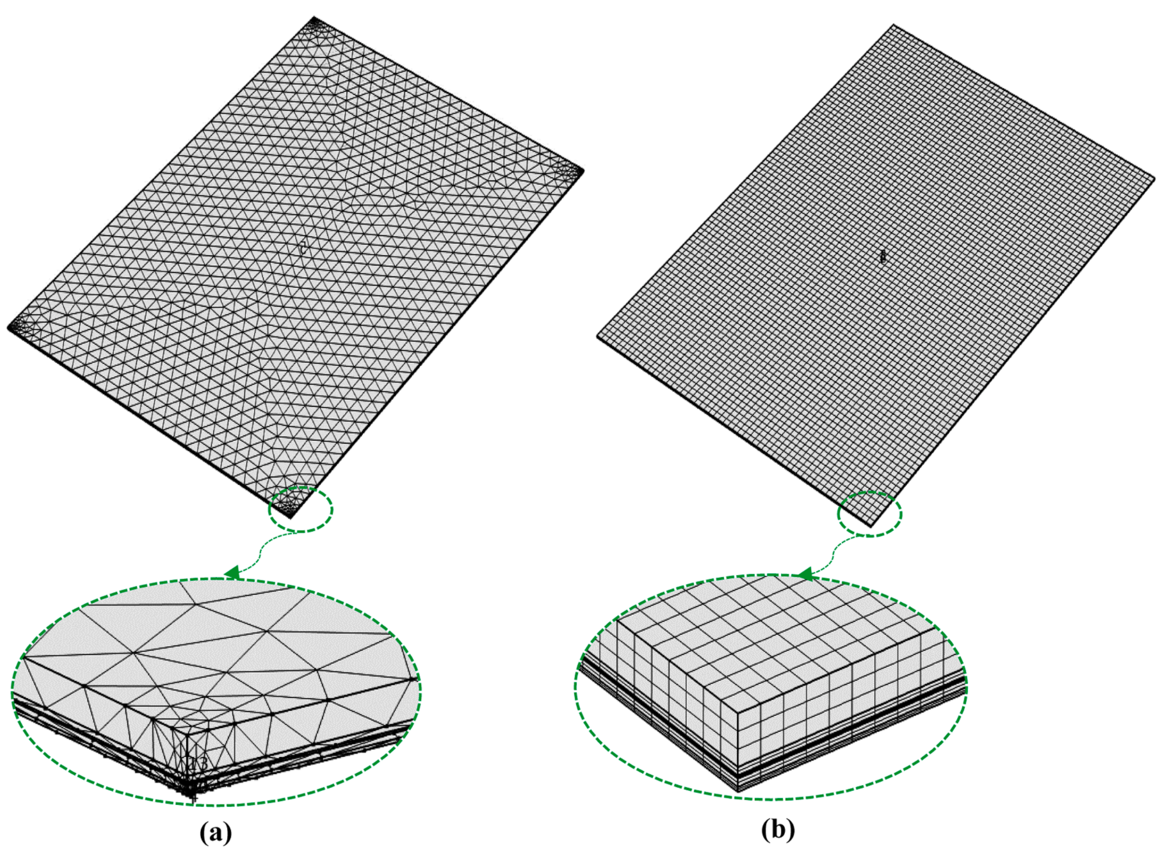

Fig. 3. (a) structured and (b) unstructured mesh of PV panel.

Table 2
Mesh independence analysis for unstructured and structured configurations.

Mesh	Mesh type	PV module temperature (°C)	Error (%)	Elements	Time of solution (s)
Structured	Normal	62.99	–	550	7
	Fine	62.86	0.20	858	7
	Finer	62.79	0.11	1881	7
	Extra fine	62.79	0.00	4147	10
	Extremely fine	62.79	0.00	12,650	39
Unstructured	Normal	62.80	–	53,370	52
	Fine	62.80	0.00	163,539	526
	Finer	62.79	0.01	993,852	2064
	Extra fine	62.79	0.00	7285,461	5821
	Extremely fine	62.79	0.00	9467,391	8053

2.7. Model validation and comparison

2.7.1. Comparison I

For the numerical model validation, a SEAC60T-300 polycrystalline PV panel was studied under actual climatic conditions in the city of El Jadida, Morocco (Fig. 4). An experiment was conducted for getting temperatures on module's front and rear faces. These data were then fed into the simulation software, enabling a comparison between numerical and experimental results to assess any discrepancies. Fig. 5a illustrates the good agreement between the two sets of results, with minor differences clearly highlighted in Fig. 5b These discrepancies can be explained by the simplifying assumptions adopted in the numerical model, such as the neglect of certain environmental parameters like humidity or rapid variations in climatic conditions. Such deviations are to be expected, as it is difficult to accurately reproduce the complexity of real-life conditions in simulation. On the other hand, the PV front temperature was found lower than the rear from the experiment This behavior can be explained by the thinness of the Tedlar layer and its limited thermal conductivity. This observation is consistent with the temperature distribution numerically (Fig. 6), confirming proposed model's reliability.

Fig. 7 displayed comparative analysis of PV's thermal distribution obtained by simulation and that measured experimentally using an infrared camera. In both configurations, the module's central area has mximum temperature, for thermal accumulation and convection limited to two directions. Conversely, the edges appear cooler because they benefit from convection in three directions. The agreement observed among the numerical and experimental results approves the proposed model's robustness and consistency.

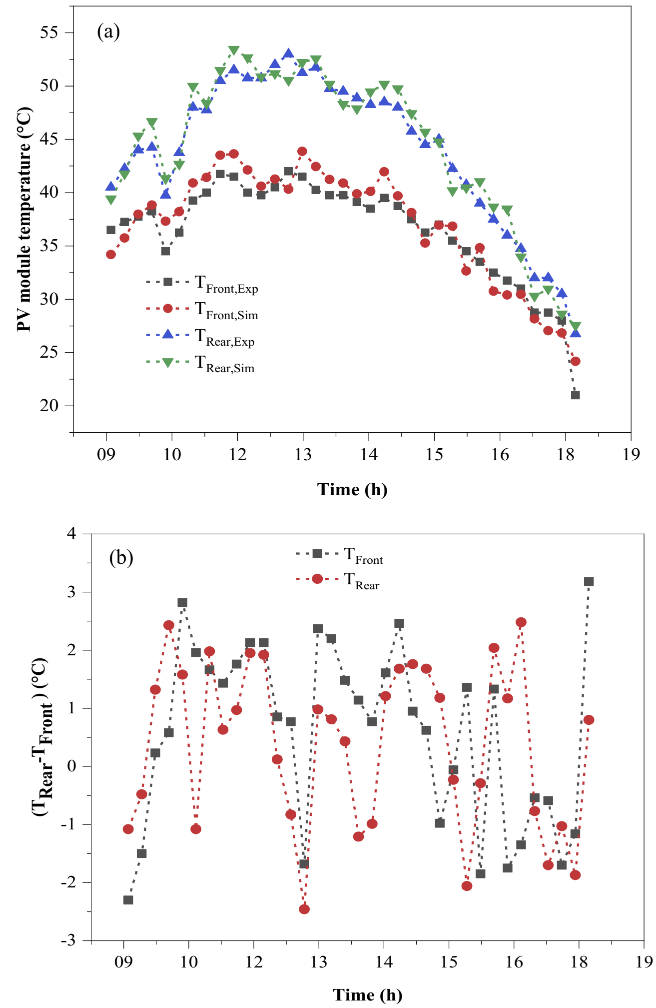

Fig. 5. Comparison between simulated and experimental temperatures (a) and the difference between the two results (b) for the PV module.

2.7.2. Comparison II

A comparison was made with several methods of predicting PV

Fig. 4. Real view of the SEAC60T-300 polycrystalline PV panel installed in El Jadida.

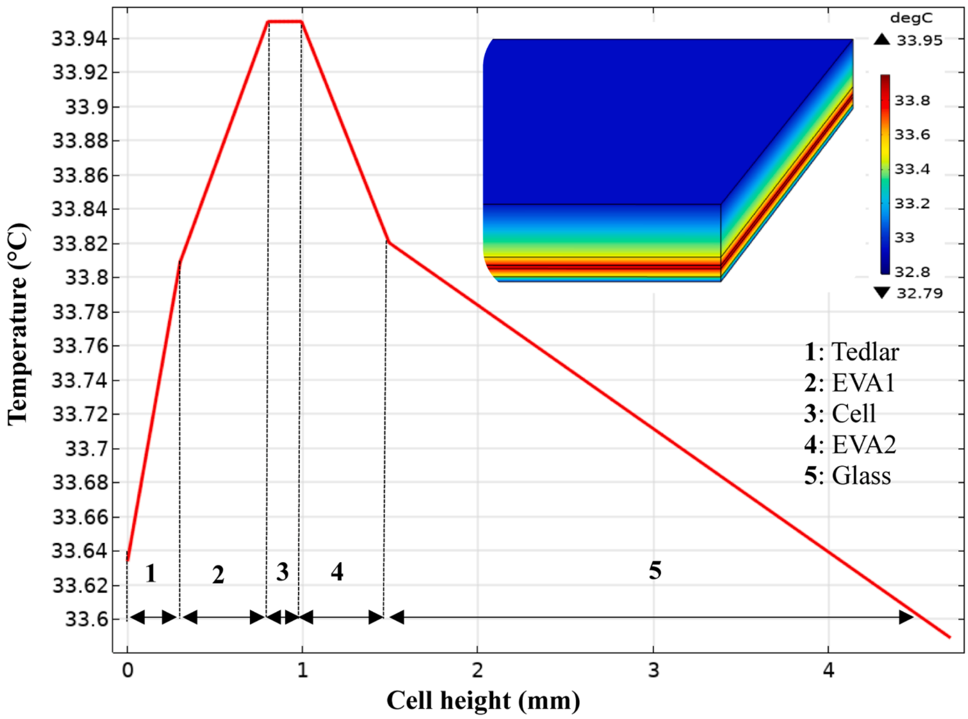

Fig. 6. Temperature variation in the PV transverse plane with $G = 200\ W/m^2$.

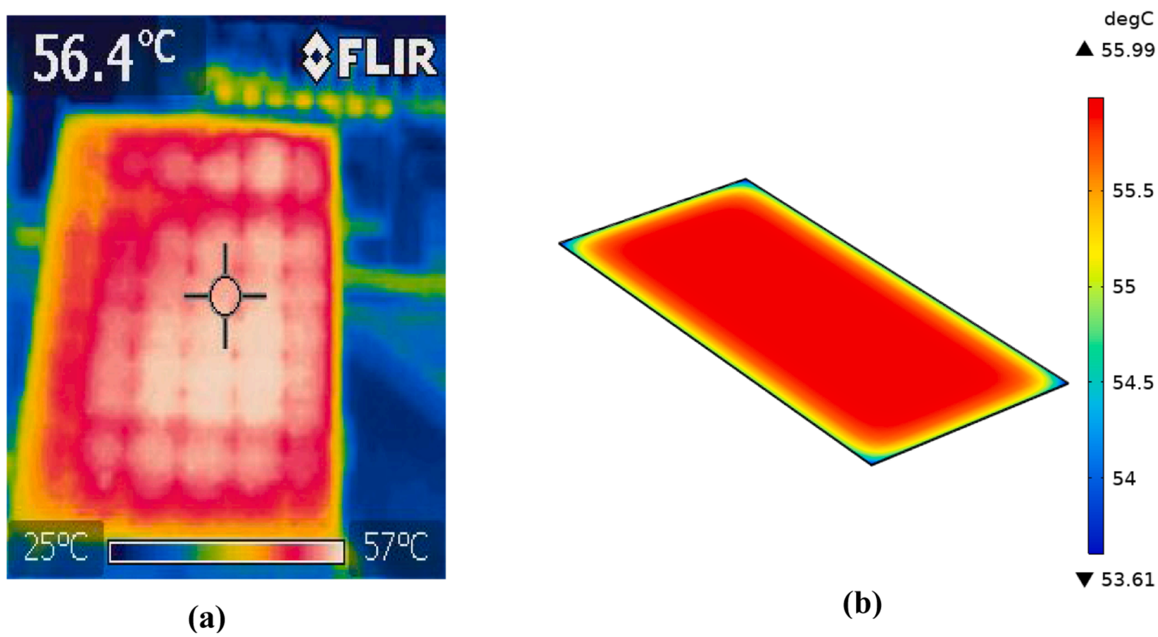

Fig. 7. Comparison of PV's thermal distribution obtained from experimental infrared camera (a) and numerical simulation (b).

module temperature (Table 3). The NOCT model in reference [24] provides a easy method to calculate module temperature at standard circumstances. However, it overlooks key factors like dust gathering, air speed, and inclination, limiting its accuracy in real-world scenarios. Other models mentioned in references [25,32,48,50] use advanced software such as COMSOL Multiphysics and ANSYS to simulate module thermal dynamics, but they differ in the number and type of parameters included. Some consider only one or two environmental factors, which limits their accuracy.

The model developed in this study makes a significant contribution by offering a comprehensive approach that simultaneously considers several environmental parameters, including ambient temperature, tilt angle, solar radiation, dust, and wind speed. This broader consideration allows us to go beyond conventional models, most of which focus solely on irradiance and temperature, leading to sometimes limited predictions. By integrating all of these variables, the proposed modeling offers an extra accurate depiction of PV module's thermal distribution, as well as a more reliable estimate of their electrical output under real operating conditions. The major advantage, therefore, lies in its ability to accurately describe the combined effect of several factors that are often overlooked in conventional approaches. However, this comprehensive approach may also involve greater complexity in

Table 3
Comparison of temperature estimation methods for solar modules.

Author	Year	Model name	Characteristics
Davis et al. [24]	2001	NOCT model	It evaluates the module's temperature in a real-life scenario, integrating the effects of irradiation and external temperature.
Zhou et al. [48]	2015	3D numerical model using ANSYS	It analyzes the polycrystalline PV temperature, considering wind velocity, external temperature, and irradiation.
Dabaghzadeh et al. [32]	2019	3D numerical model using COMSOL	The model considers wind velocity, direction, and inclination in PV thermal analysis.
Jha et al. [25]	2019	3D numerical model using COMSOL	It considers the impacts of dust and wind on module temperature.
El Alami et al. [50]	2025	3D numerical model using COMSOL	It illustrates the impact of a semi-arid climate on temperature and module performance.
This research	2025	3D numerical model using COMSOL	It investigates the influences of external temperature, irradiation, dust accumulation, air velocity, and tilt angle on PV performance.

implementation and increased dependence on the quality of input data, which is a potential limitation compared to simpler models that are less demanding in terms of data.

3. Results and discussion

Evaluating the combined impacts of several environmental parameters on the PV thermal-electrical behavior is the target of this research. To this end, five main factors were considered: solar irradiance, the PV surface's dust accumulation, external temperature, wind velocity, and inclination. These parameters were chosen because of their direct impact on the operation of PV systems under real-life conditions. To cover a wide range of situations, irradiance was varied from 200 to 1000 W/m^2, ambient temperature from 20 °C to 32 °C, wind speed from 1 m/s to 5 m/s, tilt angle from 0° to 80°, and dust deposited on the panel from 0 to 45 g/m^2. The analysis focused on the evolution of module temperature, electrical power generated, and electrical efficiency as a function of these different parameters. The results obtained provide a better understanding of the system's behavior under different climatic conditions, and details of each scenario studied are presented in the preceding sections.

3.1. Influence of dust accumulation

When dust particles accumulate on the surface of PV modules, they form a layer that limits the transmission of solar radiation through the glass, thus altering the module's thermal conditions. The result is a change in the module's temperature, power output, and electrical efficiency. Figs. 9, 10, and 11 illustrate these effects under different irradiances, assuming an ambient temperature of 26 °C, a wind speed of 2 m/s, and a zero angle of inclination.

The presence of dust on the surface of PV modules directly influences their thermal behavior. Contrary to the idea that dirt causes overheating, the results show the opposite trend: module temperature decreases as the amount of dust increases. This trend is clearly illustrated in Fig. 8, which shows the temperature distribution recorded by the FLIR camera for a clean and a dusty module. Fig. 9 shows the evolution of module temperature as a function of dust deposition rate, for irradiance up to 1000 W/m^2. For example, at an irradiance of 1000 W/m^2, the temperature of a clean module reaches 62.79 °C. When a dust layer is present at densities of 5, 15, 25, 35, and 45 g/m^2, the temperature drops to 62.27 °C, 61.96 °C, 61.78 °C, 61.68 °C, and 61.61 °C, respectively. Although these variations are small, they reveal a gradual cooling of up to 1.18 °C. This phenomenon is explained by the filtering effect of dust: by absorbing, diffusing, and reflecting part of the sun's radiation, it reduces the irradiance incident on the module, thus lowering its operating temperature.

Fig. 10 effectively illustrates the influence of dust buildup on the PV power. The data shows a progressive decline in power correlated with increasing dust levels. Specifically, at 1000 W/m^2 irradiation, a clean PV generates an output of 61,840 W. On the other hand, this value drops to 51.902 W, 45.912 W, 42.577 W, 40.571 W, and 39.235 W for dust deposition levels of 5, 15, 25, 35, and 45 g/m^2, respectively. These results correspond to power losses of 9939 W, 15,928 W, 19,263 W, 21,269 W, and 22,605 W compared with a clean module. This marked reduction happens for the attenuation of incident irradiation due to dust deposit, which acts as an optical filter. The reduction in light energy reaching the PV cells thus leads to a direct drop in electrical energy conversion.

Fig. 11 shows a slightly surprising trend in PV electrical efficiency versus dust accretion. Contrary to the usual trend of decreasing performance, PV efficiency enhances slightly with the amount of dust deposited. At 1000 W/m^2 irradiation, clean PV efficiency is 11.420 %. This rises progressively to 11.452 %, 11.471 %, 11.482 %, 11.488 % and 11.493 % for deposits of 5, 15, 25, 35, and 45 g/m^2, respectively. This apparent improvement happened due to PV's lower temperature, which induced the presence of dust. By reducing the absorption of solar radiation, dust limits module heating, which may slightly improve electrical efficiency, as cell performance is thermally sensitive. However, this increase in efficiency does not compensate for the sharp drop in power output observed, confirming that the overall effect of dust remains detrimental to energy production.

3.2. Wind velocity impact

Under 1000 W/m^2 radiation with 26 °C temperature (ambient) and 0° module tilt angle, the air speed's effect on dusty PV module's behaviour was investigated. The results, presented in Figs. 12, 13, and 14, show how module temperature, power output, and electrical efficiency change against air speed and dirt level.

Fig. 12 shows that the temperature of the PV module decreases with increasing wind speed, whether the module is clean or dust-covered. At 1 m/s wind velocity, clean PV temperature is 62.79 °C. For dusty PV of 5, 15, 25, 35, and 45 g/m^2 layer, the corresponding temperatures are 62.27 °C, 61.96 °C, 61.78 °C, 61.68 °C, and 61.61 °C, respectively. Similarly, at 5 m/s wind velocity, clean module temperature drops to 47.25 °C, while that of the dusty modules is 46.91 °C, 46.70 °C, 46.59 °C, 46.52 °C, and 46.47 °C, respectively, depending on the dust load. These results underline the wind-induced cooling effect, which contributes to lower module temperatures and improved electrical efficiency.

Fig. 13 illustrates the effect of wind speed on the electrical power generated by a PV module, whether clean or subject to different levels of dust accumulation. It can be seen that electrical power increases with wind speed, regardless of the module's cleanliness. Specifically, at a wind speed of 1 m/s, the electrical power of a clean module reaches 61.840 W. On the other hand, for modules with increasing levels of dust accumulation, respectively 5 g/m^2, 15 g/m^2, 25 g/m^2, 35 g/m^2 and 45 g/m^2, power gradually decreases, reaching 51.902 W, 45.912 W, 42.577 W, 40.571 W and 39.235 W. This is due to the reduction in incident irradiance caused by the partial obstruction of the module's active surface by dust particles. When the wind speed increases to 5 m/s, the electrical power of the clean module rises to 67.050 W, a significant gain over the situation at 1 m/s. The polluted modules also show an improvement in power output, although the values are still lower than those of the clean module. The power levels recorded are 56.213 W, 49.694 W, 46.066 W, 43.887 W, and 42.434 W, respectively, for the aforementioned dust levels.

Fig. 14 illustrates the evolution of the electrical efficiency of PV

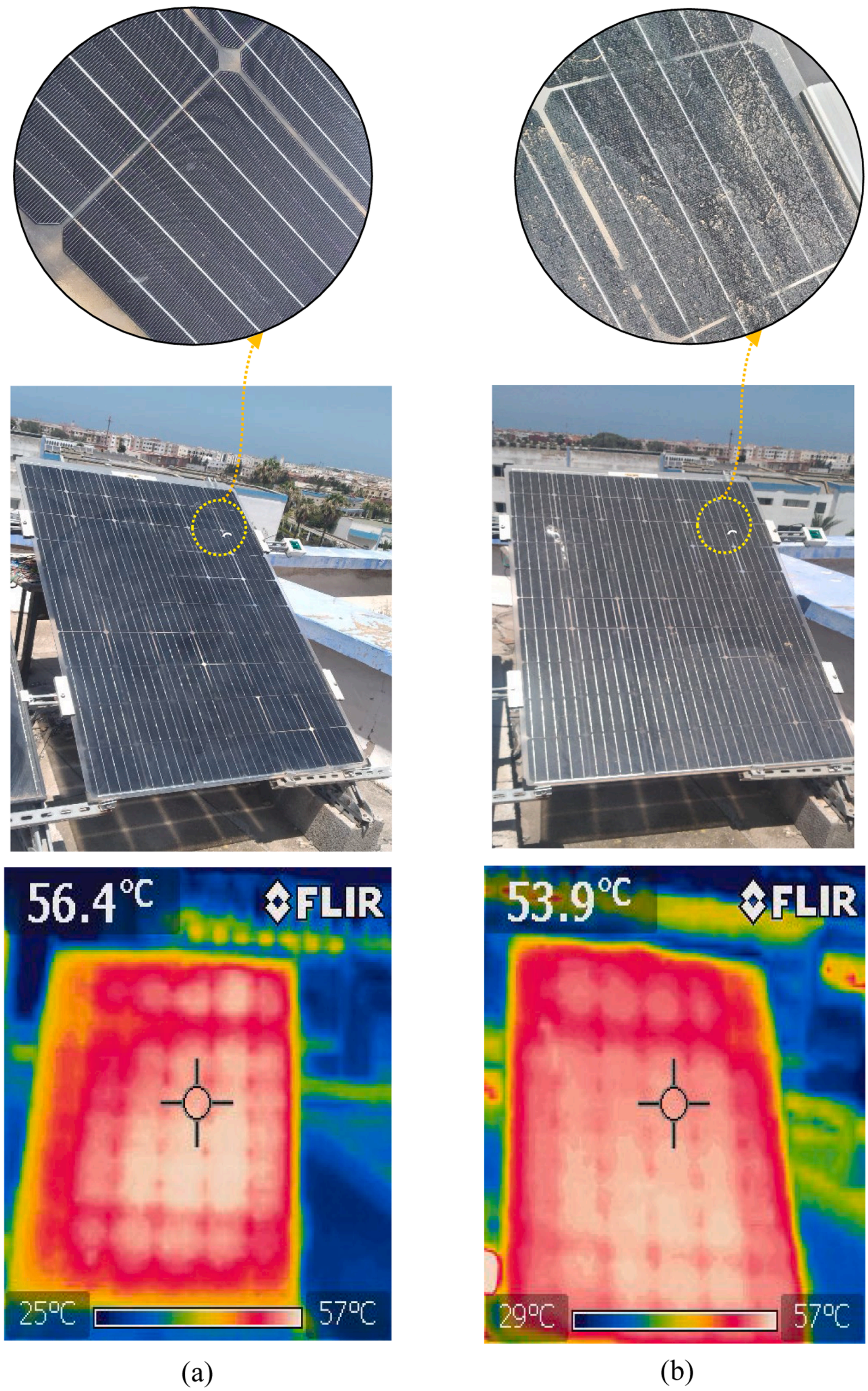

Fig. 8. Temperature distribution recorded by the FLIR camera for the PV of clean (a) and dusty (b).

modules as a function of wind speed, considering different levels of dust accumulation on their surface. It can be seen that, whatever the degree of pollution, electrical efficiency increases with wind speed. This trend is explained by the improved cooling of the modules at higher wind speeds, which reduces the operating temperature of the PV cells and thus optimizes their electrical performance. At a wind speed of 1 m/s, the electrical efficiency of a clean module is 11.420 %. For modules with dust accumulations of 5 g/m^2, 15 g/m^2, 25 g/m^2, 35 g/m^2, and 45 g/m^2,

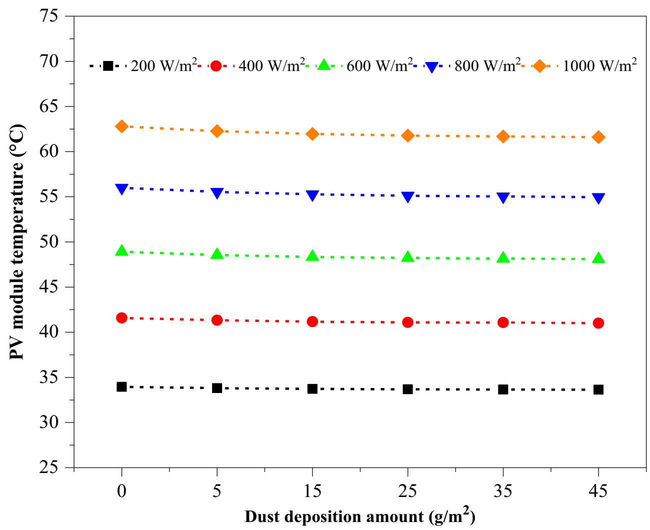

Fig. 9. Module temperature versus dust deposition due to irradiance values (200 to 1000 W/m²).

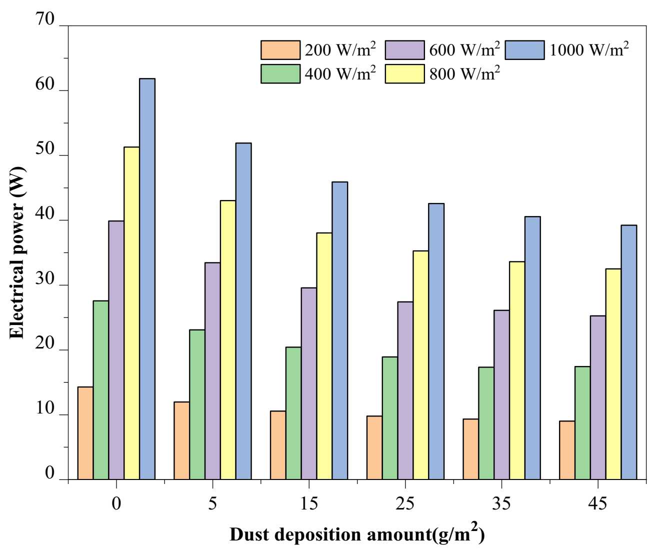

Fig. 10. Influence of dust buildup on PV power for irradiance (200–1000 W/m²).

there is a slight gradual increase in efficiency, to 11.452 %, 11.471 %, 11.482 %, 11.488 % and 11.493 % respectively. When the wind speed rises to 5 m/s, the electrical efficiency of the clean module rises to 12.382 %, reflecting a significant gain thanks to improved cooling. Similarly, for modules polluted at the above levels, efficiencies increase slightly, reaching 12.403 %, 12.416 %, 12.423 %, 12.427 % and 12.430 %.

In conclusion, wind speed has a significant contribution to PV cooling, promoting convective thermal transfer between the PV and external air. This mechanism helps to reduce module temperatures, thereby improving their energy performance. Wind can also facilitate the partial detachment of accumulated dust particles, reducing their shielding effect on solar radiation. Nevertheless, the cooling effectiveness is contingent on a combination of issues like the amount of dust deposited, irradiance, angle of inclination, and ambient temperature. It is therefore vital for investors and planners to take these effects into account when designing PV systems, to avoid oversizing, optimize costs, and determine the optimum tilt angle, thus guaranteeing maximum energy efficiency.

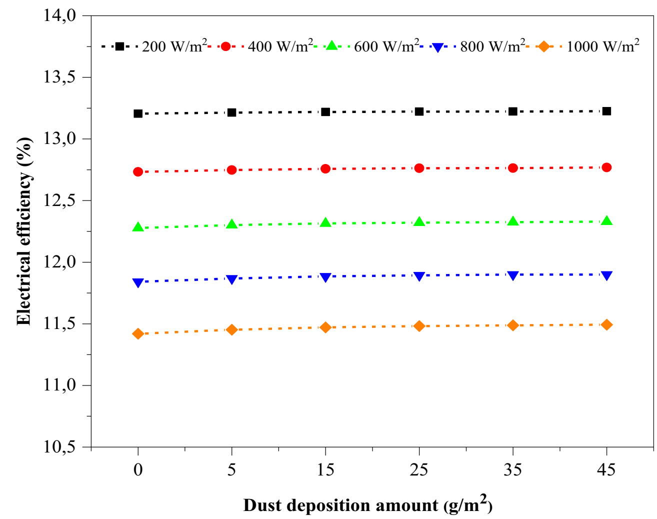

Fig. 11. Variation in PV efficiency against dust accumulation and irradiation (200 to 1000 W/m²).

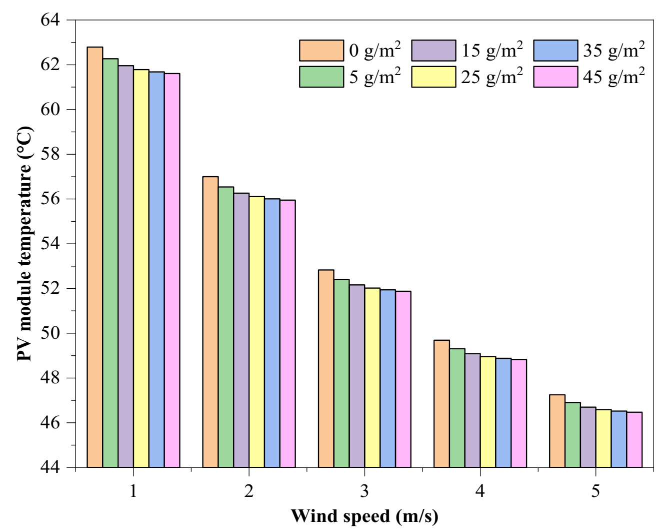

Fig. 12. PV temperature variation against wind speed and degree of dust pollution.

3.3. Inclination impact

The tilt angle of the PV module significantly influences both the amount of radiation received and heat dissipation. By adjusting this angle, it is possible to optimize the amount of solar energy captured while facilitating cooling through natural convection, which directly impacts the module's electrical efficiency. Fig. 15 illustrates the effect of tilt on the temperature distribution of a module with a wind speed of 1 m/s, an outside temperature of 26 °C, radiation of 1000 W/m², and no dust (0 g/m²). The results show that the module temperature decreases as the tilt angle increases. This reduction can be explained by two complementary effects. A greater tilt improves air circulation around the module, thereby enhancing convective cooling. The direct incident irradiance on the module surface decreases slightly at more pronounced angles, which also helps to limit heating. These observations highlight that even a change of a single degree can have a significant impact on temperature and efficiency. Optimizing the tilt angle is a strategic lever for balancing solar radiation capture and module cooling, enabling an optimal compromise between energy production and thermal control.

Fig. 16 illustrates the combined effect of tilt angle and level of dust

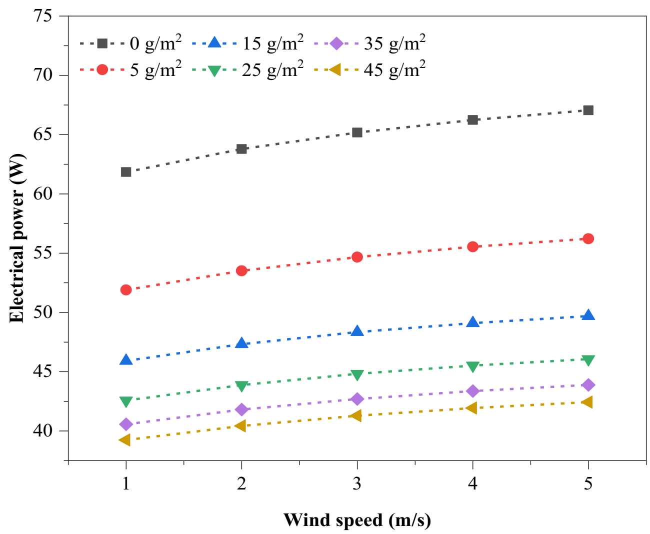

Fig. 13. Wind velocity impact on PV power subjected to various dust accumulations.

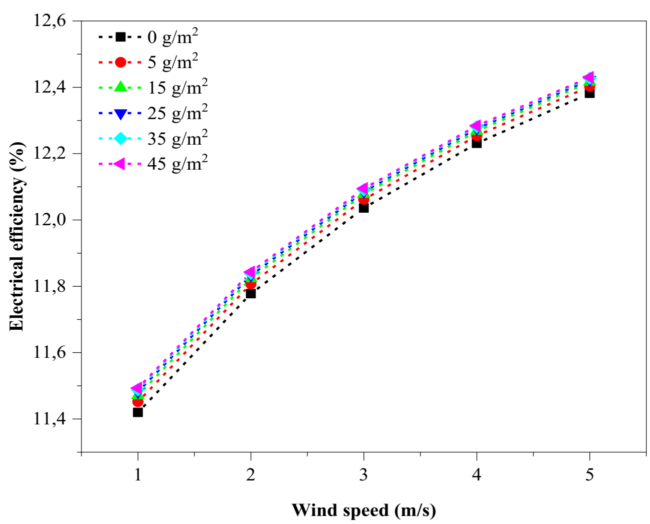

Fig. 14. Wind velocity impact on PV electrical efficiency subjected to various dust accumulations.

accumulation on PV module temperature. In general, it can be seen that module temperature decreases progressively with increasing tilt angle, whether the module is clean or subject to varying degrees of soiling. Specifically, at an angle of inclination of 0°, the temperature of a clean module reaches 62.79 °C. Where dust accumulation is present, the temperatures recorded decrease slightly with increasing dust mass, reaching 62.27 °C for 5 g/m², 61.96 °C for 15 g/m², 61.78 °C for 25 g/m², 61.68 °C for 35 g/m², and 61.61 °C for 45 g/m², respectively. This corresponds to a maximum difference of 1.18 °C between the clean module and the dirtiest module at 0° inclination. This slight decrease can be attributed to the partial reduction in irradiance absorbed by the module due to dust-induced shading. Conversely, at an angle of inclination of 80°, the temperature of the clean module falls to 36.37 °C, a significant drop of 26.42 °C compared to the temperature measured at 0° For soiled modules, the temperatures observed at this angle are also lower, with values of 35.70 °C for 5 g/m², 35.30 °C for 15 g/m², 35.08 °C for 25 g/m², 34.94 °C for 35 g/m², and 34.85 °C for 45 g/m². The maximum difference between the clean module and the dirtiest is 1.52 °C, slightly higher than at 0°, reflecting the greater effect of dust at higher angles of inclination, although the overall temperature remains significantly lower.

The electrical power generated by a PV module is strongly influenced by its tilt angle and the degree of dirtiness of its surface. Fig. 17 illustrates this dual influence. As the angle of inclination increases, power output decreases for all levels of dirt accumulation. At low inclination (0°), performance is optimal. The clean module delivers 61,840 W. However, the presence of dust reduces this value significantly, with 51.902 W for 5 g/m² of dust, then 45.912 W for 15 g/m², 42.577 W for 25 g/m², 40.571 W for 35 g/m², and finally 39.235 W for 45 g/m². When the angle reaches 80°, the drop in power becomes drastic. The module itself delivers just 12.275 W, a loss of >49 W compared to the initial angle. This trend is confirmed for soiled modules: at the same angle, power drops to 10.307 W for 5 g/m², 9.120 W for 15 g/m², 8.457 W for 25 g/m², 8.060 W for 35 g/m², and 7.795 W for 45 g/m². These results clearly show that optimizing the installation angle and regular module maintenance are two key factors in guaranteeing satisfactory power production, especially in environments exposed to dust.

Fig. 18 shows the combined effect of tilt angle and dust accumulation level on the electrical efficiency of a PV module. It can be seen that efficiency increases progressively with increasing tilt angle, whether the module is clean or dirty. The main reason for this improvement is the reduction in module operating temperature as the tilt angle increases, leading to better electrical performance. At an angle of 0°, the electrical efficiency of the clean module is 11.420 %. In the presence of dust, efficiency rises slightly with deposited mass, reaching 11.452 % for 5 g/m², 11.471 % for 15 g/m², 11.482 % for 25 g/m², 11.488 % for 35 g/m², and 11.493 % for 45 g/m², respectively. When the angle of inclination reaches 80°, the efficiency of the clean module rises to 13.055 %, a significant increase of 1.635 % compared to the initial angle of 0° For soiled modules, the same trend is observed, with respective efficiencies of 13.097 % for 5 g/m², 13.122 % for 15 g/m², 13.135 % for 25 g/m², 13.144 % for 35 g/m², and 13.150 % for 45 g/m². These results indicate that increasing the angle of inclination not only partially compensates for dirt losses but also improves overall electrical efficiency, mainly through module cooling.

3.4. Irradiation impact

Solar irradiance is a decisive parameter in the amount of energy received by the surface of PV modules, directly influencing their operating temperature. Fig. 19 shows the temperature distribution on the surface of a PV module subjected to different irradiance intensities, under fixed conditions: wind speed of 1 m/s, ambient temperature of 26 °C, zero inclination (0°), and no dust on the surface (0 g/m²). The results show a progressive rise in module temperature with increasing irradiance. The peripheral areas of the module also show lower temperatures, due to greater convective heat loss, favored by exposure to air on three sides. By contrast, temperatures are significantly higher in the center of the module, as confirmed by images taken by the FLIR camera (Figs. 7 and 8). This can be explained by the more limited heat dissipation in this region, where convective exchange with the environment takes place in only two directions, resulting in greater thermal accumulation.

Fig. 20 shows the effect of solar irradiance and dust accumulation on the temperature of PV modules. It is seen that module temperature rises significantly with escalating irradiation. It happens as a small proportion of the incident irradiation is transformed into electricity via the photoelectric phenomenon. The rest of the absorbed energy is converted into heat, raising the temperature of the module when this heat is not dissipated efficiently. The figure also shows that clean modules systematically have higher temperatures than dirty ones. The accumulation of dust slightly reduces the solar energy absorbed, thus limiting heating. For example, at an irradiance of 200 W/m², the temperature of the clean module reaches 33.95 °C. With increasing dust accumulation, temperatures drop slightly, with 33.81 °C for 5 g/m², 33.73 °C for 15 g/m², 33.68 °C for 25 g/m², 33.66 °C for 35 g/m², and 33.64 °C for 45 g/m². At higher irradiance levels, i.e., 1000 W/m², the same phenomenon is more

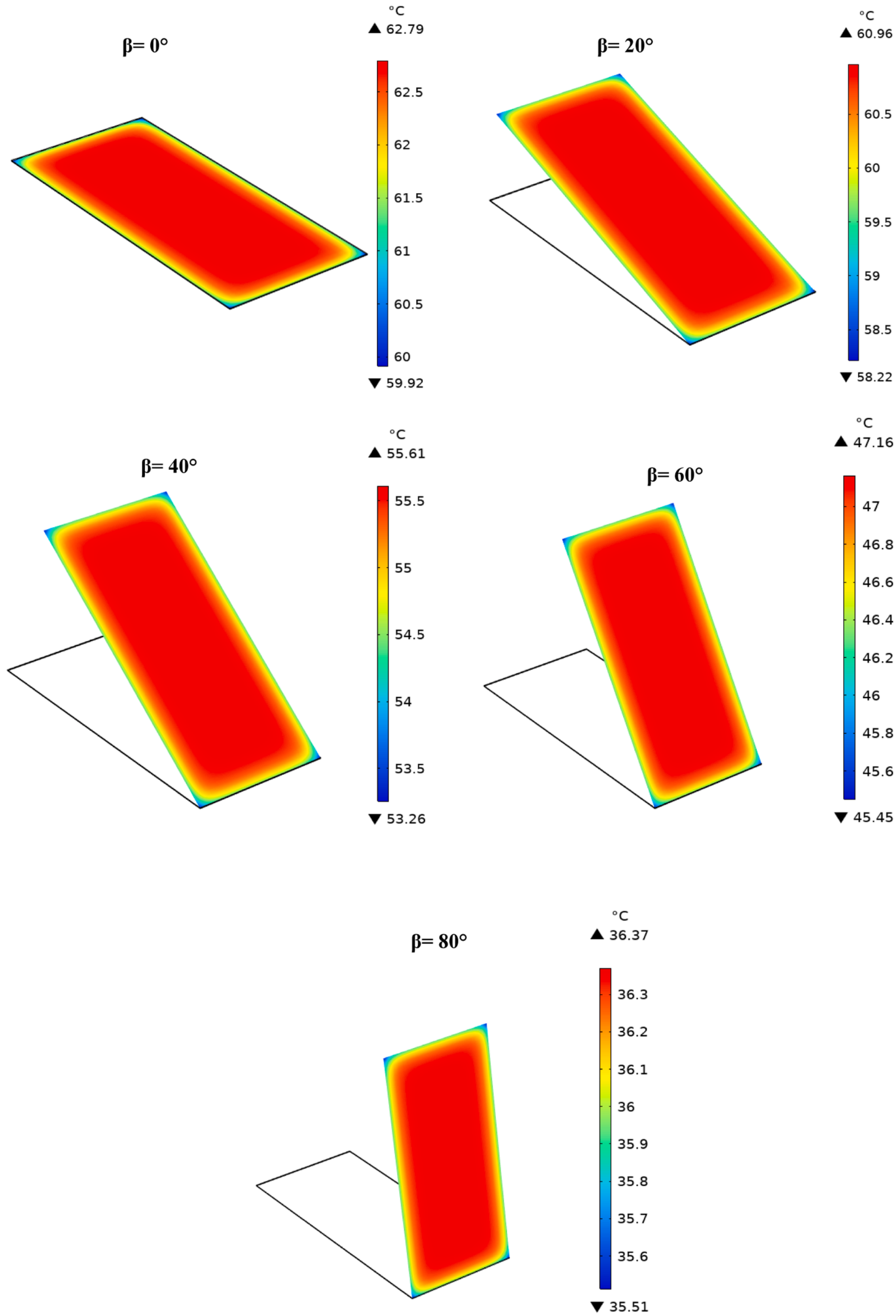

Fig. 15. Effect of tilt angle on PV thermal distribution.

marked. The temperature of the clean module reaches 62.79 °C. In the presence of dust, this temperature falls progressively, reaching 62.27 °C for 5 g/m^2, 61.96 °C for 15 g/m^2, 61.78 °C for 25 g/m^2, 61.68 °C for 35 g/m^2, and 61.61 °C for 45 g/m^2. These results confirm that increasing irradiance intensifies PV module heating and that the presence of dust, while reducing energy efficiency, has a moderating effect on temperature by reducing solar radiation absorption.

Fig. 21 shows the relationship between solar irradiance and the electrical power generated by PV modules, considering the effect of soiling. Generally speaking, the power generated increases as irradiance rises. This trend can be explained by the fact that more intense solar irradiance provides more usable energy, which in turn increases the current generated by the PV effect. However, the presence of dust on the module surface reduces the incident energy absorbed, thus limiting electricity production. For example, at an irradiance of 200 W/m^2, the clean module delivers a power of 14.301 W. However, this power drops to 11.977 W for an accumulation of 5 g/m^2, then to 10.581 W for 15 g/m^2, 9.805 W for 25 g/m^2, 9.339 W for 35 g/m^2, and 9.028 W for 45 g/m^2. At a higher irradiance of 1000 W/m^2, the same trend is observed, with greater variations. Clean module power then reaches 61.840 W, while power levels recorded for increasing levels of soiling are 51.902 W for 5 g/m^2, 45.912 W for 15 g/m^2, 42.577 W for 25 g/m^2, 40.571 W for 35 g/m^2, and 39.235 W for 45 g/m^2.

Fig. 22 shows the evolution of the electrical efficiency of PV modules

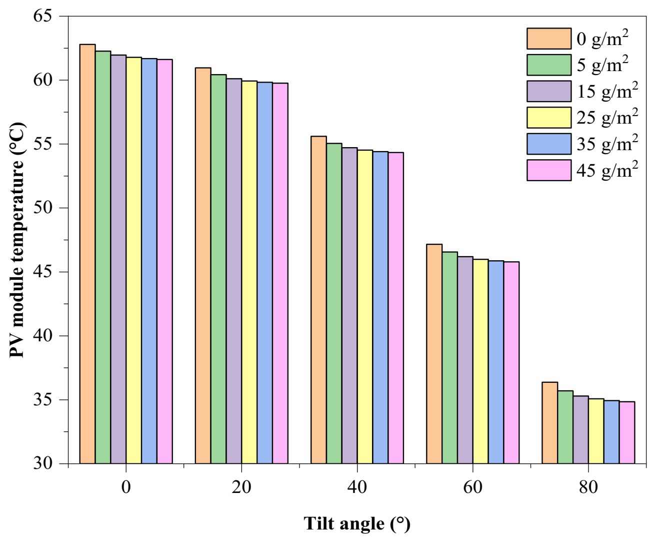

Fig. 16. Evolution of PV temperature against tilt angle, and dust accumulation.

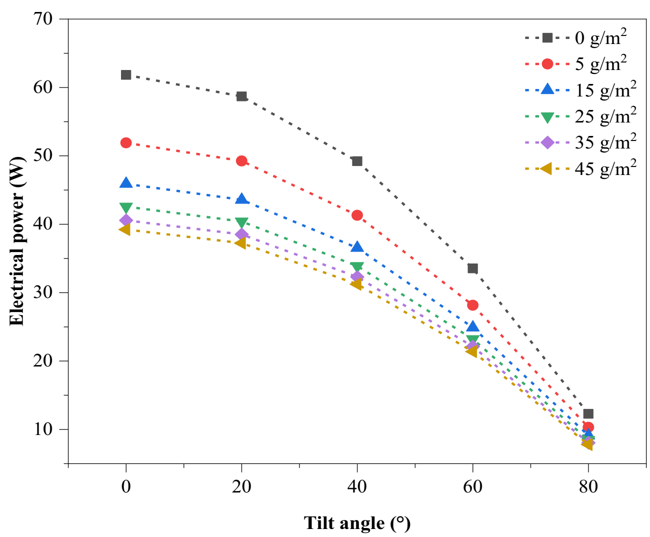

Fig. 17. PV electrical power versus angle of inclination and dust buildup layer.

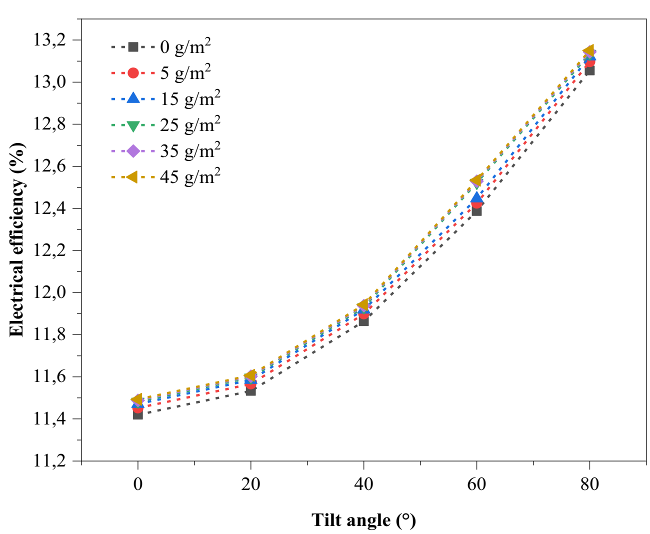

Fig. 18. PV efficiency depending on inclination and dust deposited amount.

as a function of solar irradiance and the level of dust accumulation. Contrary to the trend observed for electrical power, efficiency decreases as irradiance increases. This is because, at high levels of solar irradiance, a greater proportion of the energy absorbed is converted into heat rather than electricity, resulting in a rise in module temperature and, consequently, a drop in conversion efficiency. At low irradiance, e.g., 200 W/m², the clean module efficiency reaches 13.205 %. This efficiency increases slightly in the presence of dust, reaching 13.214 % for 5 g/m², 13.219 % for 15 g/m², 13.222 % for 25 g/m², 13.223 % for 35 g/m², and 13.225 % for 45 g/m². This slight increase is due to the reduction in thermal rise, as dust partially limits the absorption of radiation. On the other hand, at a higher irradiance of 1000 W/m², the efficiency of the clean module drops to 11.420 %. For soiled modules, a similar trend is observed, with efficiencies of 11.452 % for 5 g/m², 11.471 % for 15 g/m², 11.482 % for 25 g/m², 11.488 % for 35 g/m², and 11.493 % for 45 g/m².

3.5. *Influence of ambient temperature*

Figs. 23, 24, and 25 show the influence of ambient temperature on PV module temperature, generated power, and electrical efficiency, considering several levels of dust accumulation, a wind speed of 1 m/s, a zero-tilt angle (0°), and an irradiance of 1000 W/m².

Fig. 23 clearly illustrates that PV module temperature increases almost linearly with ambient temperature, regardless of the level of dust accumulation. This temperature rise adversely affects module performance, as it reduces their conversion efficiency. As a result, PV modules generally perform better in winter, when lower ambient temperatures keep the module's operating temperature at a moderate level. This trend is consistent with results presented in previous work [25,50], which report slightly higher energy production in winter under equivalent irradiance conditions. The moderating effect of dust on module temperature can also be observed. At an ambient temperature of 20 °C, the temperature of the clean module reaches 57.78 °C. At 5 g/m², 15 g/m², 25 g/m², 35 g/m² and 45 g/m² dust buildup, this temperature gradually decreases to 57.24 °C, 56.91 °C, 56.72 °C, 56.61 °C and 56.54 °C. At 32 °C external temperature, the clean PV registers 67.82 °C temperature. For dust accumulations of 5, 15, 25, 35, and 45 g/m², the temperatures measured are slightly lower, reaching 67.32 °C, 67.03 °C, 66.86 °C, 66.76 °C, and 66.69 °C, respectively.

Fig. 24 shows an almost linear decrease in PV module electrical output with increasing ambient temperature. This phenomenon is mainly explained by the negative impact of rising temperature on PV cell efficiency, due to an increase in charge carrier recombination and a drop in open-circuit voltage. Dust accumulation on the module surface also acts as a power-reducing factor by reducing the incident irradiance received by the cells. At an ambient temperature of 20 °C, the maximum power of a clean module is 63.519 W. This power decreases significantly as dust accumulates, falling to 53.312 W for 5 g/m², then to 47.165 W, 43.737 W, 41.679 W and finally 40.307 W for accumulations of 15, 25, 35 and 45 g/m² respectively. When the ambient temperature rises to 32 °C, there is a general drop in power, with 60.151 W for the clean module and reduced values of 50.484 W, 44.655 W, 41.412 W, 39.462 W, and 38.160 W for the same dust levels.

Fig. 25 shows an almost linear decrease in PV module electrical efficiency with increasing ambient temperature. This can be explained by the negative thermal effect on the electrical characteristics of the PV cells, in particular, the reduction in open-circuit voltage due to the temperature rise. Indeed, at an ambient temperature of 20 °C, the efficiency of the clean module is 11.730 %, while it increases slightly with dust, reaching 11.763 % for 5 g/m² and peaking at 11.807 % for 45 g/m² of accumulation. Similarly, at 32 °C, the efficiency of the clean module is 11.108 %, rising gradually with dust to 11.178 % at 45 g/m².

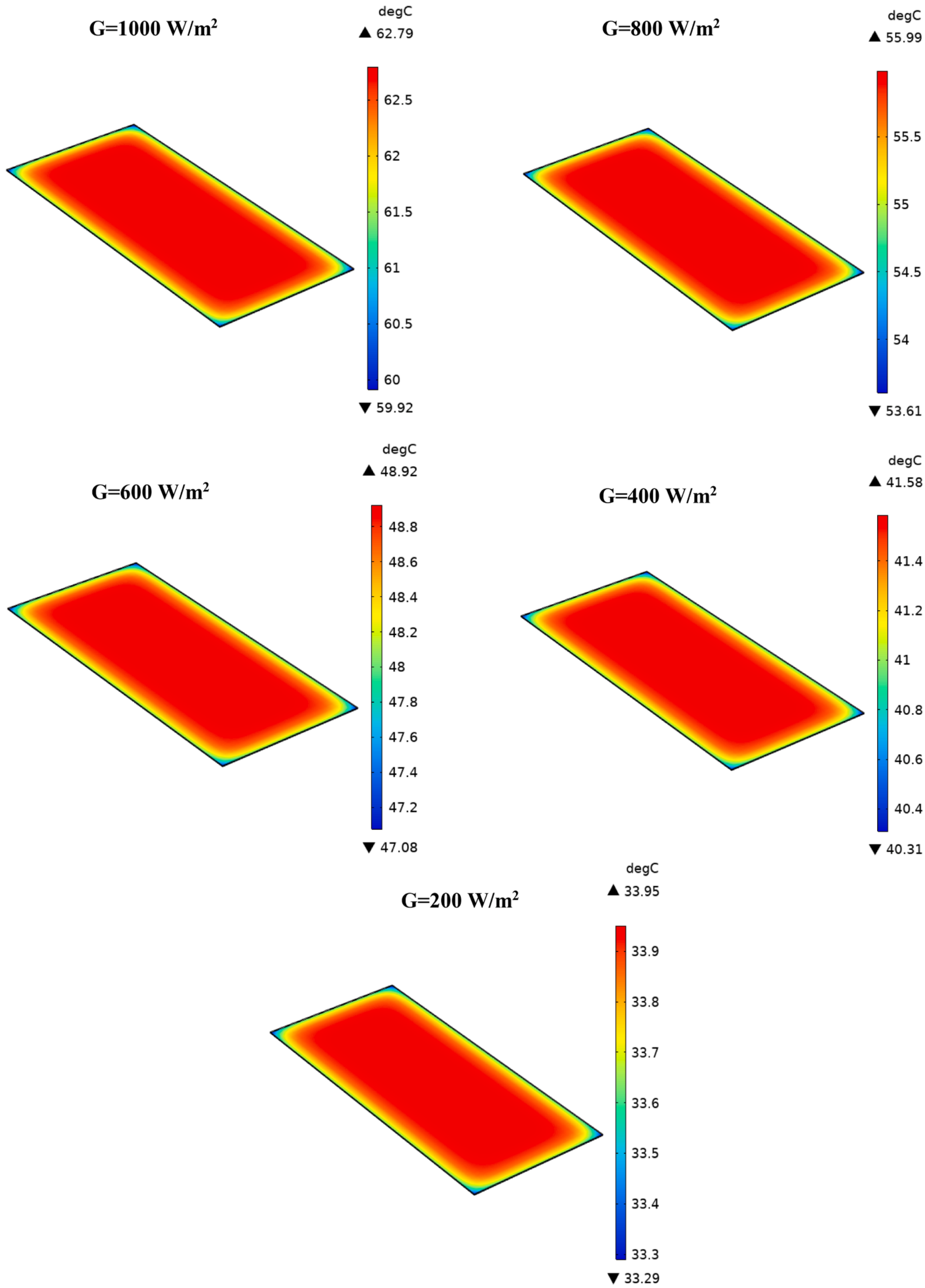

Fig. 19. PV thermal distribution at different irradiation levels.

3.5. *Grey relational analysis (GRA)*

To select the parameters that have the greatest influence on the performance of a PV module, an analysis based on the grey relational method developed by Deng in 1982 was conducted [51], considering five environmental factors, namely irradiance, ambient temperature, wind speed, tilt angle, and dust quantity. This method makes it possible to evaluate the proximity of variation of each parameter in relation to the output variable, whether it be the temperature of the module, its electrical power, or its efficiency, using the Grey Relational Degree, after normalization over the interval [0–1]. The use of this method over other analytical techniques is justified by its simplicity of implementation, ease of calculation [52], and effectiveness in evaluating multiple response functions and ranking alternatives, making it particularly suitable for multi-criteria decision-making [53]. Nevertheless, this method has certain limitations since it does not provide a causal explanation, limiting itself to identifying the relative importance of factors, and the results may vary depending on the normalization method adopted.

The steps for determining the Grey Relational Degree (GRD) involve

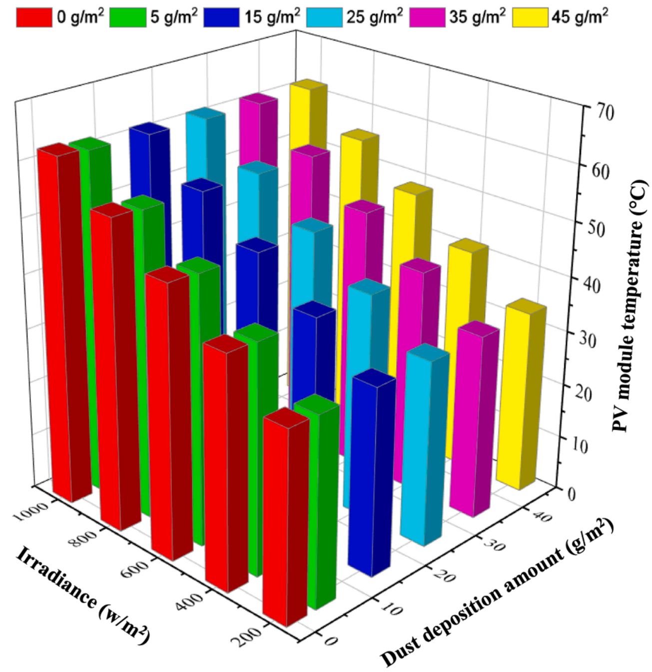

Fig. 20. Dust buildup and irradiance versus PV temperature.

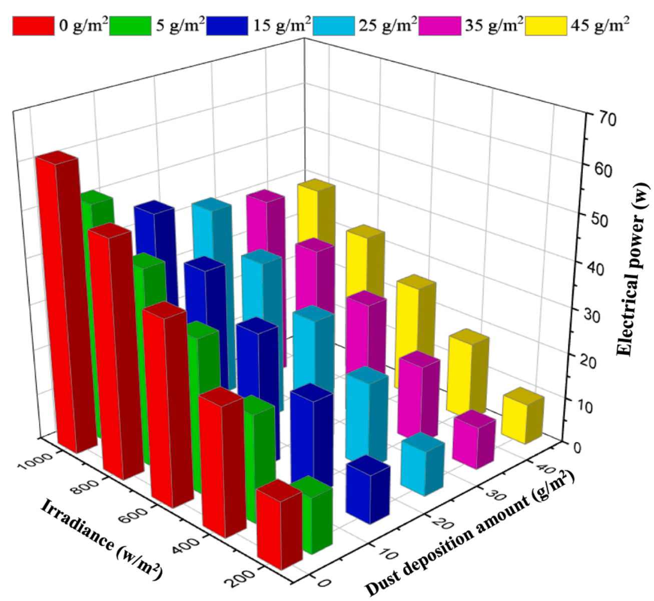

Fig. 21. PV power versus irradiation and soiling level.

normalizing the data, as the factors have different units and must be made comparable. Either the "the larger, the better" approach or the "the smaller, the better" approach can be used. The "smaller is better" approach (Eq. (11)) was applied to the responses relating to the temperature of the PV modules, while the "bigger is better" approach (Eq. (12)) was used for the responses relating to electrical power and efficiency [53]. Next, the difference between the reference series, corresponding to the normalized output variable, and each compared series corresponding to a normalized factor is determined, and then the gray relational coefficient (GRC) of each analyzed sequence is calculated (Eq. (13)). Finally, the GRD is calculated and ranked in descending order to define a criterion for evaluating the importance of the factors (Eq. (14)) [52–54].

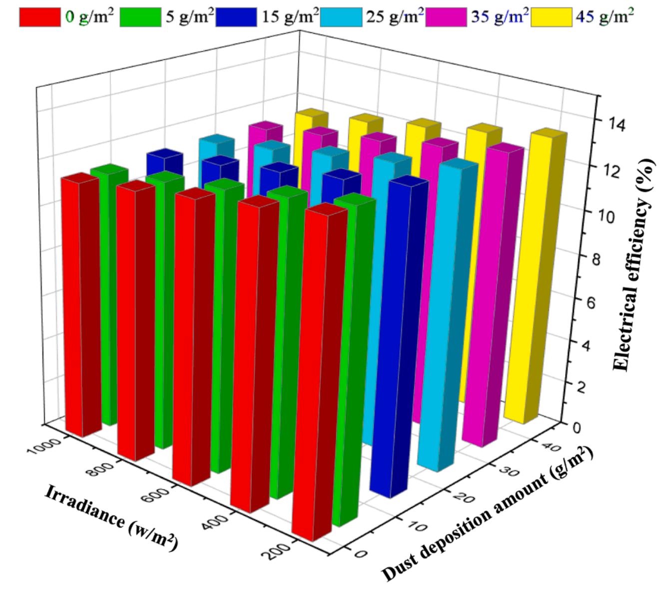

Fig. 22. PV efficiency versus irradiation intensity and dust deposited amount.

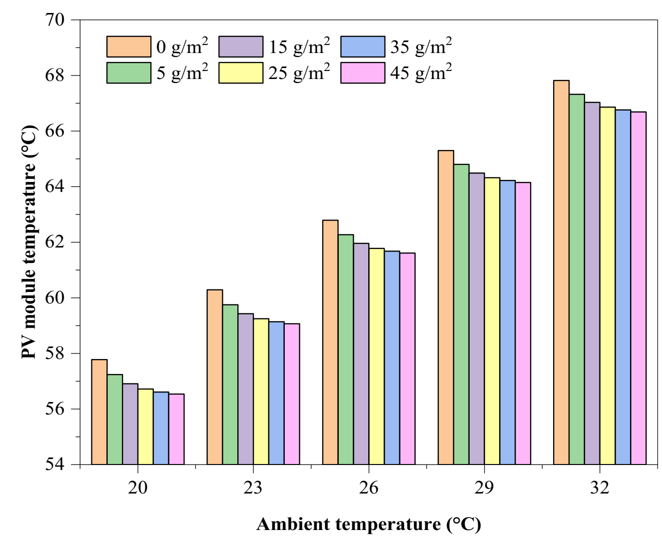

Fig. 23. PV temperature against external temperature for various dust amounts.

$$x_{ij} = \frac{\max(y_{ij}) - y_{ij}}{\max(y_{ij}) - \min(y_{ij})} \tag{11}$$

$$x_{ij} = \frac{y_{ij} - \min(y_{ij})}{\max(y_{ij}) - \min(y_{ij})} \tag{12}$$

where y_{ij} is the original response corresponding to the test number and the considered variable, and x_{ij} is the normalized response with a value ranging from 0 to 1. $\max(y_{ij})$ represents the highest value for each considered response, while $\min(y_{ij})$ corresponds to the lowest possible value for these responses.

$$GRC = \frac{\Delta_{\min} + \xi \cdot \Delta_{\max}}{\Delta + \xi \cdot \Delta_{\max}} \tag{13}$$

where ξ represents the identification coefficient, typically assigned a

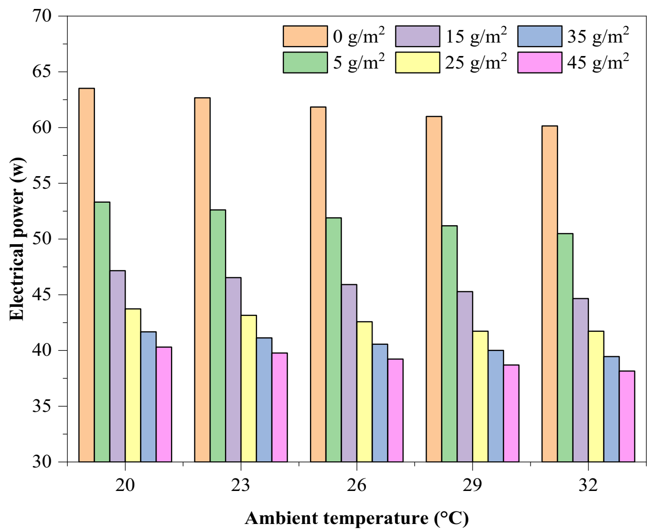

Fig. 24. Variation of PV module power output according to ambient temperature and dust load.

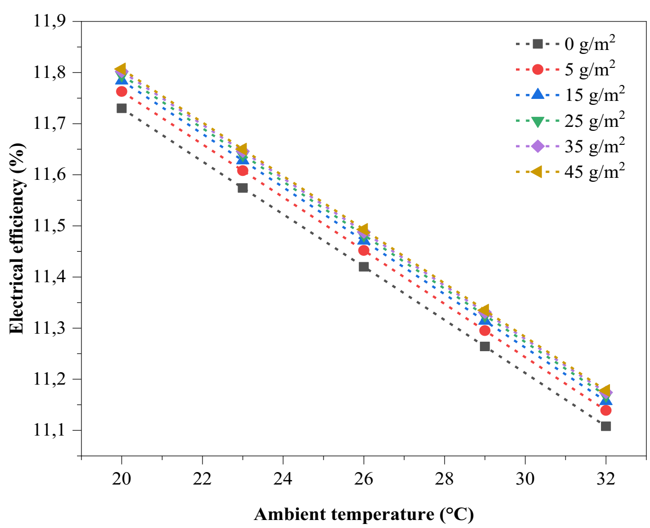

Fig. 25. Variation in PV module electrical output against dust load and external temperature.

value of 0.5 [54].

$$GRD = \frac{1}{n}\left(\sum_{i=1}^{n} GRC\right) \quad (14)$$

The results show that dust is the most influential parameter on all the indicators studied (Table 4). It has a grey relationship of 0.5476 for module temperature, 0.6878 for electrical power, and 0.6820 for electrical efficiency, placing it in first place in all rankings. This strong correlation can be attributed to the fact that the accumulation of dust on the module surface acts simultaneously as an obstacle to the transmission of solar radiation and as a thermal insulator that slows down heat dissipation, thus directly impacting the thermal and electrical behavior of the system. In comparison, other parameters such as irradiance, ambient temperature, wind speed, and tilt angle show similar GRD values for each indicator, i.e., 0.5446 for temperature, 0.5474 for electrical power, and 0.5964 for efficiency. This reflects a moderate and balanced influence of these factors on module performance.

From a practical point of view, these results highlight the need to implement effective strategies to limit dust accumulation on modules, for example, through regular cleaning, to maintain a good level of energy performance. Furthermore, although their individual impact is less pronounced, other environmental parameters must also be considered in prediction and sizing models, because of their combined effect on overall module behavior.

4. Conclusion

This study proposes an original approach based on the three-dimensional modeling of heat transfer in PV modules, considering several physical and environmental parameters. The model developed has been validated through comparison with experimental data, demonstrating its reliability. The model's performance has also been compared with that of other models in the literature, highlighting its strengths in terms of accuracy. The model was used to assess the effects of various factors, including dust buildup, wind velocity, solar irradiance, installation angle, and external temperature, on the PV system's working temperature, energy efficiency, and power output. Additionally, an analysis based on the Grey Relation Degree method was conducted to prioritize the influence of five key parameters on overall system performance. This approach represents an innovative contribution to this research. The main findings are presented below:

- The presence of dust alters the PV thermal-electrical behavior. At 1000 W/m^2, compared to a module covered with 45 g/m^2 of dust, a clean module has a 1.18 °C higher temperature (62.79 °C vs. 61.61 °C), a 22.605 W (57.6 %) higher power output, and a 0.073 % lower efficiency (11.420 % vs. 11.493 %). These results show that, although dust induces a slight gain in efficiency due to module cooling, it results in a significant loss of energy, confirming its overall negative impact on performance.
- Increasing wind speed from 1 to 5 m/s reduces PV module temperature by around 15 °C, from 62.79 °C to 47.25 °C for a clean module, and from 61.61 °C to 46.47 °C for a very dusty module (45 g/m^2). This drop in temperature results in an increase in electrical efficiency, from 11.42 % to 12.38 % for a clean module, and from 11.49 % to 12.43 % for a dusty module. At the same time, electrical power output is always higher for clean modules, but increases with wind speed for all dust levels.
- The angle of inclination has a strong influence on the temperature and power of PV modules: at low inclination, the temperature is high (62.79 °C) with maximum power (61,840 W) that gradually

Table 4
Degrees of grey relationship for factors influencing PV temperature, power, and efficiency.

	0–1 Interval normalization					
	GRD on temperature		GRD on power		GRD efficiency	
Factors	GRD	Correlation Ranking	GRD	Correlation Ranking	GRD	Correlation Ranking
Dust (g/m^2)	0.5476	1	0.6878	1	0.6820	1
Irradiance (W/m^2)	0.5446	2	0.5474	2	0.5964	2
Tilt angle (°)	0.5446	2	0.5474	2	0.5964	2
Wind speed (m/s)	0.5446	2	0.5474	2	0.5964	2
Ambient temperature (°C)	0.5446	2	0.5474	2	0.5964	2

decreases with dust. At high tilt (80°), the temperature drops (36.37 °C), but the power output drops drastically (down to 12,275 W for a clean module).

- Ambient temperature has a strong influence on PV module performance. When the ambient temperature rises from 20 °C to 32 °C, the clean module temperature increases from 57.78 °C to 67.82 °C, resulting in a drop in power output from 63.519 W to 60.151 W. Dust accumulation plays a moderating role on temperature, reducing it by up to 1.24 °C at 32 °C for 45 g/m^2, but results in a marked drop in power, down to 23.212 W at 20 °C.
- The increase in solar irradiance causes an almost linear rise in the temperature of PV modules, reaching 62.79 °C at 1000 W/m^2 for a clean module. This thermal rise results in a decrease in electrical power, which drops from 61.840 W to 39.235 W as dust levels increase from 0 to 45 g/m^2. At the same time, electrical efficiency rises slightly, from 11.420 % to 11.493 %, thanks to the slight cooling induced by the dust.
- According to the GRA method, the amount of dust deposited has the greatest influence on the temperature, power, and efficiency of the PV module, followed by irradiance, ambient temperature, wind speed, and tilt angle.

This study shows that dust accumulation, wind speed, tilt angle, solar radiation, and ambient temperature have a significant impact on module temperature and the electrical output of PV panels. Based on this, several practical recommendations can be made to improve the design and maintenance of PV systems. During the design phase, it is advisable to select an optimal tilt angle and position the modules to promote natural heat dissipation and minimize the formation of hot spots. Real-time monitoring of panel temperature and performance enables the rapid identification of any anomalies and facilitates an effective response. For maintenance, it is recommended to keep the modules clean through regular cleaning operations and, if possible, to use automated solutions to limit dust accumulation and maximize efficiency. These combined measures help to extend the life of the modules, maintain high energy efficiency, and ensure optimal operation of the installations under real-world conditions.

5. Future work

Based on the results of this study, several research prospects can be considered. First, the numerical model developed could be extended to be applied to a wider range of PV technologies, such as PERC, bifacial, and thin-film modules. Assessing the effects of dust and soiling on these different technologies, as well as studying their long-term aging, will provide a better understanding of the specific vulnerabilities and advantages of each material. In addition, it would be useful to incorporate climate variability by applying the model to various environments (desert, coastal, or urban areas) in order to identify the most critical conditions. Another avenue is to optimize maintenance strategies by using this model to propose predictive cleaning schedules, while analyzing the economic consequences of dust and maintenance on the cost of ownership of PV systems. Finally, extending the study to hybrid systems, such as PVT panels, would provide a more comprehensive understanding of the impact of environmental conditions on the simultaneous production of electricity and heat.

CRediT authorship contribution statement

Yassine El Alami: Writing – original draft, Visualization, Validation, Software, Methodology, Formal analysis, Data curation, Conceptualization. **Elhadi Baghaz:** Writing – review & editing, Validation, Supervision, Funding acquisition, Data curation. **Rehena Nasrin:** Writing – review & editing, Validation, Methodology, Investigation. **Charaf Hajjaj:** Writing – review & editing, Visualization, Investigation, Data curation. **Mohammadi Benhmida:** Writing – review & editing, Investigation, Data curation. **Khaled M. Al-Aribe:** Writing – review & editing, Supervision, Funding acquisition. **Adnan Ibrahim:** Writing – review & editing, Investigation, Formal analysis, Data curation, Conceptualization.

Declaration of competing interest

The authors declare that they have no known competing financial interests or personal relationships that could have appeared to influence the work reported in this paper.

Data availability

Data will be made available on request.

References

[1] S. Minazhova, M. Kurrat, B. Ongar, A. Georgiev, Deploying a rooftop PV panels in the southern regions of Kazakhstan, Energy 320 (2025) 135205, https://doi.org/10.1016/j.energy.2025.135205.
[2] Y. El Alami, E. Baghaz, R. Nasrin, M. Al-Damook, R. Bendaoud, T. Bouragba, M. Melhaoui, M. Benhmida, Up-to-date review on flat-plate solar hybrid photovoltaic Thermal systems: absorber designs and fabrication materials, Int. J. Energy Res. 2025 (2025) 5547555, https://doi.org/10.1155/er/5547555.
[3] Y. El Alami, E. Chetouani, H. Mokhliss, F. Ouerradi, M. Aoutoul, S. Bounouar, R. Bendaoud, A. Faize, R. Rmaily, Optimizing solar energy efficiency with an improved hill-climbing maximum power point tracking control approach: hardware implementation, Clean Energy 8 (2024) 167–176, https://doi.org/10.1093/ce/zkae061.
[4] A. Gulraiz, S.S.H. Zaidi, H. Gulraiz, B.M. Khan, M. Ali, B. Khan, Leveraging dense layer hybrid graph neural networks for managing overvoltage in PV-dominated distribution systems, Results Eng 27 (2025) 106169, https://doi.org/10.1016/j.rineng.2025.106169.
[5] Y.E. Alami, E. Baghaz, R. Nasrin, S. Padmanaban, M. Louzazni, Numerical approach of an advanced hybrid photovoltaic thermal system based on exergy, energy, enviro-economic, and sustainability factors, Results Eng (2025) 106342, https://doi.org/10.1016/j.rineng.2025.106342.
[6] Y. El Alami, E. Baghaz, R. Nasrin, F. Chanaa, R. Bendaoud, S. Padmanaban, M. Louzazni, Experimental-numerical comparative study of performance and cost-effectiveness of partially- and fully-cooled photovoltaic thermal systems, Case Stud, Therm. Eng. 73 (2025) 106660, https://doi.org/10.1016/j.csite.2025.106660.
[7] J. Cai, J. Fang, M. Liang, Z. Shi, L. Xu, T. Zhang, W. Huang, Dynamic reconfiguration method and performance optimization of 3D curved photovoltaic modules under non-uniform illumination conditions based on improved simulated annealing algorithm (ISAA), Appl. Energy 393 (2025) 126162, https://doi.org/10.1016/j.apenergy.2025.126162.
[8] S.D. Farahani, M. Alibeigi, Investigation of power generated from a PVT-TEG system in Iranian cities, J. Sol. Energy Res. 5 (2020) 603–616, https://doi.org/10.22059/jser.2020.308162.1170.
[9] W. Zhao, S. Hu, Z. Dong, F. Zhao, F. Lv, X. Guan, Y. Lv, Multifactor heat transfer modeling and performance evaluation of photovoltaic modules: simulation and experimental study, Appl. Therm. Eng. 278 (2025) 127117, https://doi.org/10.1016/j.applthermaleng.2025.127117.
[10] R. Budakoğlu, D.A. Akın, O.İ. İrey, E. Gökçen, G. Kasapoğlu, D. Yılmaz, Environmentally sustainable methodology for the extraction of ethyene vinyl acetate (EVA) residue from EoL PV panel dismantled by hot knife, Renew. Energy 246 (2025) 122872, https://doi.org/10.1016/j.renene.2025.122872.
[11] C. Wang, A. Yang, J. Li, Z. Si, Experimental study on effect of multi-factor coupling on the surface temperature of photovoltaic module, Acta Energ. Sol. Sin. 40 (2019) 112–118.
[12] L. Huang, Z. Song, Q. Dong, Y. Song, X. Zhao, J. Qi, L. Shi, Surface temperature and power generation efficiency of PV arrays with various row spacings: a full-scale outdoor experimental study, Appl. Energy 367 (2024) 123362, https://doi.org/10.1016/j.apenergy.2024.123362.
[13] A. Gholami, M. Ameri, M. Zandi, R. Gavagsaz Ghoachani, S. Jafarzadegan Gerashi, H.A. Kazem, A.H.A. Al-Waeli, Impact of harsh weather conditions on solar photovoltaic cell temperature: experimental analysis and thermal-optical modeling, Sol. Energy 252 (2023) 176–194, https://doi.org/10.1016/j.solener.2023.01.039.
[14] H.H. Jo, J. Kim, S. Kim, Enhancing the power generation performance of photovoltaic system: impact of environmental and system factors, Appl. Therm. Eng. 240 (2024) 122221, https://doi.org/10.1016/j.applthermaleng.2023.122221.
[15] A. Keddouda, R. Ihaddadene, A. Boukhari, A. Atia, M. Arıcı, N. Lebbihiat, N. Ihaddadene, Experimental and numerical modeling of photovoltaic modules temperature under varying ambient conditions, Energy Convers. Manag. 312 (2024) 118563, https://doi.org/10.1016/j.enconman.2024.118563.
[16] K. Yaman, G. Arslan, A detailed mathematical model and experimental validation for coupled thermal and electrical performance of a photovoltaic (PV) module,

Appl. Therm. Eng. 195 (2021) 117224, https://doi.org/10.1016/j.applthermaleng.2021.117224.
[17] W. Zhao, Y. Lv, Q. Zhou, W. Yan, Collision-adhesion mechanism of particles and dust deposition simulation on solar PV modules, Renew. Energy 176 (2021) 169–182, https://doi.org/10.1016/j.renene.2021.05.057.
[18] R.G. Ross, Interface design considerations for terrestrial solar cell modules, in: Proceedings of the 12th IEEE Photovoltaic Specialist's Conference, Baton Rouge L. A, 1976, p. 801e806.
[19] T. Nordmann, L. Clavadetscher, Understanding temperature effects on PV system performance, in: 3rd World Conference on photovoltaic Energy Conversion, Proceedings 3, 2003, p. 2243e2246.
[20] F. Lasnier, Photovoltaic Engineering Handbook, Routledge, New York, 2017, https://doi.org/10.1201/9780203743393.
[21] J.-M. Servant, Calculation of the cell temperature for photovoltaic modules from climatic data, in: E. Bilgen, K.G.T. Hollands (Eds.), Intersol Eighty Five, Pergamon, Oxford, 1986, pp. 1640–1643, https://doi.org/10.1016/B978-0-08-033177-5.50311-2.
[22] D.L. King, Photovoltaic module and array performance characterization methods for all system operating conditions, AIP Conf Proc 394 (1997) 347–368, https://doi.org/10.1063/1.52852.
[23] D. King, J. Kratochvil, W. Boyson, W. Bower, in: Field Experience with a New Performance Characterization Procedure for Photovoltaic Arrays. 2nd World Conference and Exhibition on Photovoltaic Solar Energy Conversion, Vienna, 1998, 6-10 July 1998.
[24] M.W. Davis, A.H. Fanney, B.P. Dougherty, Prediction of building integrated photovoltaic cell temperatures, J. Sol. Energy Eng. 123 (2001) 200–210, https://doi.org/10.1115/1.1385825.
[25] A. Jha, P.P. Tripathy, Heat transfer modeling and performance evaluation of photovoltaic system in different seasonal and climatic conditions, Renew. Energy 135 (2019) 856–865, https://doi.org/10.1016/j.renene.2018.12.032.
[26] W. Gu, T. Ma, L. Shen, M. Li, Y. Zhang, W. Zhang, Coupled electrical-thermal modelling of photovoltaic modules under dynamic conditions, Energy 188 (2019) 116043, https://doi.org/10.1016/j.energy.2019.116043.
[27] M. Jaszczur, J. Teneta, Q. Hassan, E. Majewska, R. Hanus, An experimental and numerical investigation of photovoltaic module temperature under varying environmental conditions, Heat Transf. Eng. 42 (2021) 354–367, https://doi.org/10.1080/01457632.2019.1699306.
[28] J. Kim, Y. Nam, Study on the cooling effect of attached fins on PV using CFD simulation, Energies 12 (2019) 758, https://doi.org/10.3390/en12040758.
[29] Y.E. Alami, F. Ouerradi, S. Bounouar, M. Benhmida, M. Rhiat, B. Benhala, K. Hirech, E. Baghaz, Comparative study of the performance of photovoltaic and photovoltaic thermal solar systems: case study in El Jadida, E3S Web Conf. 601 (2025) 00011, https://doi.org/10.1051/e3sconf/202560100011.
[30] Y. El Alami, H.E. Achouby, E. Baghaz, C. Hajjaj, R. Nasrin, An innovative photovoltaic thermal system with direct water-cell contact: energy, exergy, and sustainability analysis, Sol. Energy 300 (2025) 113827, https://doi.org/10.1016/j.solener.2025.113827.
[31] H. Lu, W. Zhao, CFD prediction of dust pollution and impact on an isolated ground-mounted solar photovoltaic system, Renew. Energy 131 (2019) 829–840, https://doi.org/10.1016/j.renene.2018.07.112.
[32] N. Dabaghzadeh, M. Eslami, Temperature distribution in a photovoltaic module at various mounting and wind conditions: a complete CFD modeling, J. Renew. Sustain. Energy 11 (2019) 053503, https://doi.org/10.1063/1.5114895.
[33] S. Kaplanis, E. Kaplani, J.K. Kaldellis, PV temperature and performance prediction in free-standing, BIPV and BAPV incorporating the effect of temperature and inclination on the heat transfer coefficients and the impact of wind, efficiency and ageing, Renew. Energy 181 (2022) 235–249, https://doi.org/10.1016/j.renene.2021.08.124.
[34] P. Boottarat, C. Photong, An experimental study on effects of dust particle sizes on efficiency of monocrystalline solar cells, in: 2023 International Electrical Engineering Congress (iEECON), 2023, pp. 214–218.
[35] I. Morsi, The prediction of PV output power based on dust, materials' accumulation and partial shadings by using fuzzy logic control, Results Eng. 26 (2025) 105263, https://doi.org/10.1016/j.rineng.2025.105263.
[36] H.S. Abd, H.K. Judran, S.H.A. Aun, A.A. Jaddoa, K.A. Hammoodi, S.A. Kadhim, J. M. Daif, Dust deposition and cleaning effect on PV panel: experimental approach, Results Eng 27 (2025) 106041, https://doi.org/10.1016/j.rineng.2025.106041.
[37] N. Gökmen, W. Hu, P. Hou, Z. Chen, D. Sera, S. Spataru, Investigation of wind speed cooling effect on PV panels in windy locations, Renew. Energy 90 (2016) 283–290, https://doi.org/10.1016/j.renene.2016.01.017.
[38] Y. El Alami, A. Ameur, M. Benhmida, A. Rabhi, E. Baghaz, Performance evaluation of different new channel box photovoltaic thermal systems, J. Clean. Prod. 478 (2024) 143953, https://doi.org/10.1016/j.jclepro.2024.143953.
[39] A.D. Jones, C.P. Underwood, A thermal model for photovoltaic systems, Sol. Energy 70 (2001) 349–359, https://doi.org/10.1016/S0038-092X(00)00149-3.
[40] Y. Du, W. Tao, Y. Liu, J. Jiang, H. Huang, Heat transfer modeling and temperature experiments of crystalline silicon photovoltaic modules, Sol. Energy 146 (2017) 257–263, https://doi.org/10.1016/j.solener.2017.02.049.
[41] J. Singh, M. Aditya Sabbineni, R.P. Jaiswal, Internal active cooling of a crystalline silicon photovoltaic module: development of a modeling framework, Sol. Energy 264 (2023) 111980, https://doi.org/10.1016/j.solener.2023.111980.
[42] Y. El Alami, E. Baghaz, R. Bendaoud, F. Chanaa, M. Benhmida, H. Ezzaki, R. Nasrin, Experimental-numerical investigation of the photovoltaic Thermal system with polypropylene heat exchanger: case in Morocco, IET Renew. Power Gener. 19 (2025) e70041, https://doi.org/10.1049/rpg2.70041.
[43] J. Zhou, Z. Zhang, H. Liu, Q. Yi, Temperature distribution and back sheet role of polycrystalline silicon photovoltaic modules, Appl. Therm. Eng. 111 (2017) 1296–1303, https://doi.org/10.1016/j.applthermaleng.2016.10.095.
[44] Y. Lee, A.A.O. Tay, Finite element thermal analysis of a solar photovoltaic module, Energy Procedia 15 (2012) 413–420, https://doi.org/10.1016/j.egypro.2012.02.050.
[45] Y. Bannour, Y. El Alami, R. Nasrin, N. El Moussaoui, B. Elhadi, A. Faiz, Numerical optimization of fin configurations in phase change material systems for improving solar panel cooling and electrical efficiency, Energy Storage 7 (5) (2025) e70241, https://doi.org/10.1002/est2.70241.
[46] U. Olmuş, Y.E. Güzelel, K.N. Çerçi, O. Büyükalaca, Numerical analysis and comparison of different serpentine-based photovoltaic-thermal collectors, Renew. Energy 241 (2025) 122196, https://doi.org/10.1016/j.renene.2024.122196.
[47] W.C. Swinbank, Long-wave radiation from clear skies, Q. J. R. Meteorol. Soc. 89 (1963) 339–348, https://doi.org/10.1002/qj.49708938105.
[48] J. Zhou, Q. Yi, Y. Wang, Z. Ye, Temperature distribution of photovoltaic module based on finite element simulation, Sol. Energy 111 (2015) 97–103, https://doi.org/10.1016/j.solener.2014.10.040.
[49] C. Shen, Y. Zhang, C. Zhang, J. Pu, S. Wei, Y. Dong, A numerical investigation on optimization of PV/T systems with the field synergy theory, Appl. Therm. Eng. 185 (2021) 116381, https://doi.org/10.1016/j.applthermaleng.2020.116381.
[50] Y. El Alami, A. Lamkaddem, R. Nasrin, F. Ouerradi, N. El Moussaoui, F. Chanaa, E. Baghaz, Optimizing the performance of hybrid photovoltaic-thermal systems by choosing the input temperature, in: Proceedings of the 4th International Conference on Advances in Communication Technology and Computer Engineering (ICACTCE 2024), Book Chapter, Lecture Notes in Networks and Systems, Switzerland 1312, Springer Nature, 2025, pp. 1–11, https://doi.org/10.1007/978-3-031-94620-2_39.
[51] D. Ju-Long, Control problems of grey systems, Syst. Control Lett. 1 (1982) 288–294, https://doi.org/10.1016/S0167-6911(82)80025-X.
[52] N.S. Asefa, K. Shahapurkar, T. Nigussie, A.A. Hassen, M.E.M. Soudagar, Y. Fouad, I. Ali, S. Shelare, S. Sharma, V.K. Bupesh Raja, A. Mahapatro, S. Singh, A. Kumar, E. El Sayed Massoud, J. Lozanovic, Maximizing photovoltaic thermal system through computational fluid dynamics-driven multi-factor parametric optimization: a Taguchi-grey relational analysis method to enhancing electrical output and cooling efficiency for sustainable energy, Case Stud, Therm. Eng. 69 (2025) 105991, https://doi.org/10.1016/j.csite.2025.105991.
[53] A. Ustaoglu, B. Kursuncu, V. Akgül, J. Okajima, Design and performance optimization of non-imaging concentrating photovoltaic thermal systems using grey relational analysis and response surface methodology, Appl. Therm. Eng. 273 (2025) 126482, https://doi.org/10.1016/j.applthermaleng.2025.126482.
[54] D.-K. Liu, C.-C. Hsieh, T.-W. Liao, C.-F.J. Kuo, The use of the Taguchi method with Grey relational analysis for nanofluid-phase change-optimized parameter design at a rooftop solar photovoltaic thermal composite module for small households, Sustainability 15 (2023) 15163, https://doi.org/10.3390/su152015163.